AD-A126 940 A METHOD OF ACTUATOR PLACEMENT FOR VIBRATION CONTROL OF LARGE SPACE STRUCTURES(U) AIR FORCE INST OF TECH WRIGHT-PATTERSON AFB OH R E ORT FEB 83 1/1

UNCLASSIFIED AFIT/CI/NR-83-1-T F/G 22/2 NL

END
DATE
FILMED
5 -83
DTIC

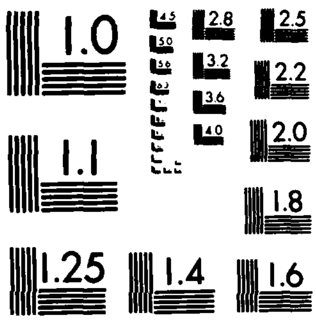

MICROCOPY RESOLUTION TEST CHART
NATIONAL BUREAU OF STANDARDS-1963-A

UNCLASS

SECURITY CLASSIFICATION OF THIS PAGE (When Data Entered)

REPORT DOCUMENTATION PAGE

READ INSTRUCTIONS BEFORE COMPLETING FORM

1. REPORT NUMBER AFIT/CI/NR-83-1T — 2. GOVT ACCESSION NO. AD-A126940	3. RECIPIENT'S CATALOG NUMBER
4. TITLE (and Subtitle) A Method of Actuator Placement for Vibration Control of Large Space Structures	5. TYPE OF REPORT & PERIOD COVERED THESIS/~~DISSERTATION~~/
	6. PERFORMING ORG. REPORT NUMBER
7. AUTHOR(s) Ricky Eugene Ort	8. CONTRACT OR GRANT NUMBER(s)
9. PERFORMING ORGANIZATION NAME AND ADDRESS AFIT STUDENT AT: Massachusetts Institute of Technology	10. PROGRAM ELEMENT, PROJECT, TASK AREA & WORK UNIT NUMBERS
11. CONTROLLING OFFICE NAME AND ADDRESS AFIT/NR WPAFB OH 45433	12. REPORT DATE Feb 83
	13. NUMBER OF PAGES 89
14. MONITORING AGENCY NAME & ADDRESS (if different from Controlling Office)	15. SECURITY CLASS. (of this report) UNCLASS
	15a. DECLASSIFICATION/DOWNGRADING SCHEDULE

16. DISTRIBUTION STATEMENT (of this Report)

APPROVED FOR PUBLIC RELEASE; DISTRIBUTION UNLIMITED

AD A126940

17. DISTRIBUTION STATEMENT (of the abstract entered in Block 20, if different from Report)

18. SUPPLEMENTARY NOTES

APPROVED FOR PUBLIC RELEASE: IAW AFR 190-17

24 Mar 83

Lynn E. Wolaver

LYNN E. WOLAVER
Dean for Research and Professional Development
AFIT, Wright-Patterson AFB OH

19. KEY WORDS (Continue on reverse side if necessary and identify by block number)

20. ABSTRACT (Continue on reverse side if necessary and identify by block number)

ATTACHED

DTIC FILE COPY

DTIC SELECTE APR 19 1983 S E D

DD FORM 1 JAN 73 1473 EDITION OF 1 NOV 65 IS OBSOLETE

UNCLASS

SECURITY CLASSIFICATION OF THIS PAGE (When Data Entered)

83 04 19 007

83-1

A METHOD OF ACTUATOR PLACEMENT FOR
VIBRATION CONTROL OF LARGE SPACE STRUCTURES

by

RICKY EUGENE ORT

B.S., The Pennsylvania State University
(1979)

SUBMITTED IN PARTIAL FULFILLMENT
OF THE REQUIREMENTS FOR THE
DEGREE OF

MASTER OF SCIENCE IN
AERONAUTICS AND ASTRONAUTICS

at the
MASSACHUSETTS INSTITUTE OF TECHNOLOGY
FEBRUARY, 1983

Signature of Author *Ricky Eugene Ort*
Department of Aeronautics and Astronautics
December 22, 1982

Approved by *E. Fogel*
Technical Advisor, CSDL

Certified by *Bruce K. Walker*
Thesis Supervisor

Accepted by ____________________
Chairman, Departmental Graduate Committee

I hereby assign my copyright of this thesis to The Charles Stark Draper Laboratory, Inc., Cambridge, Massachusetts.

Permission is hereby granted by The Charles Stark Draper Laboratory, Inc. to the Massachusetts Institute of Technology to reproduce any or all of this thesis.

S 2-1

A METHOD OF ACTUATOR PLACEMENT FOR VIBRATION CONTROL OF LARGE SPACE STRUCTURES

by

RICKY E. ORT

1st Lt. UNITED STATES AIR FORCE

Submitted to the Department of
Aeronautics and Astronautics on December 23, 1982
in partial fulfillment of the requirements for the
degree of Master of Science
in Aeronautics and Astronautics

ABSTRACT

This thesis presents several computationally simple techniques for choosing actuator placement on large space structures. Actuator and performance information can be represented as vectors (node shapes) in modal coordinates. The placement problem is stated as choosing a set of actuator node shapes to match the performance node shape. One method sequentially selects a set of actuator node shapes such that the norm of the component orthogonal to the already selected set is large. Another method sequentially selects actuator node shapes such that a large projection is obtained along the least squares residual vector resulting from the fit of the previously selected set to the performance node shape. These techniques are applied to a 100 meter cantilever beam. Good control authority over the primary modes is demonstrated. The second technique is modified to place actuators to achieve good control authority on primary modes while minimizing spillover effect. It is demonstrated that proper placement of actuators can limit spillover effect to selected modes.

Technical Supervisor: Eliezer Fogel, CSDL

Thesis Supervisor: Bruce Walker
Title: Assistant Professor of
Aeronautics and Astronautics

49 PAGES

ACKNOWLEDGMENT

I would like to thank my technical advisor, Dr. Eliezer Fogel, of the Charles Stark Draper Laboratory for his help and suggestions throughout the research and writing of this thesis. I would also like to thank my thesis advisor, Dr. Bruce Walker, for his helpful comments on the thesis text.

TABLE OF CONTENTS

TABLE OF CONTENTS (Cont.)

CHAPTER 1

INTRODUCTION

1.1 Background

The addition of the space shuttle to the present booster fleet will allow orbital insertion of much larger structures than previously possible. These structures are generically termed large space structures (LSS). The dimensions of LSS being considered for future applications are on the order of 20 meters to several hundred meters, with some estimates ranging as high as several kilometers[1,2]. Possible applications range from telescope systems to solar power satellites.

LSS are characterized as being lightweight, flexible, and having little natural damping. These structures tend to have very low natural vibration frequencies. This effect, coupled with low damping ratios due to a lack of a viscous medium like atmosphere, causes the system to have long energy decay times. This feature makes the control design very difficult.

The LSS control problem can be broken into three broad categories; attitude control, vibration control, and shape control[3]. As a practical matter, simultaneous control of two or all three functions may be required. Attitude control for a satellite or space vehicle means the orientation or pointing of the rigid body modes. Vibration control for LSS means the damping of vibration modes. Shape control for LSS means the maintenance of a portion or all of the LSS surface contour to a prescribed shape. A satellite or a space vehicle can be defined as a LSS if the attitude control system or other structural disturbances induce vibrations in the structure which are large enough to deteriorate the vehicle performance (e.g. line of sight error) or in the more extreme

case cause shape distortion. Thus, in order for a LSS to have adequate performance there must be vibration control.

The tools of modern control theory such as Linear-Quadratic-Gaussian (LQG) control theory can be effectively applied to the vibration control problem, however some modifications are required[4]. LSS are essentially distributed parameter systems that should be described via partial differential equations. In practice, the dynamics of a structure are analyzed using finite element techniques. This leads to a LSS model which is composed of a large number of second order differential equations. Unfortunately, the order of the model is too high for practical use of LQG control synthesis. This is due to the numerical difficulty of solving the control equations[5] and the inaccuracy of the finite element model at high frequencies[6]. A common approach to overcome this problem is to design the controller using a reduced order model, say by choosing a set of modes most important to performance (termed here primary modes)[7,8]. The controller so designed is subsequently applied to the full order system. This leads to the undesirable interaction of the controller with the ignored modes which in turn can lead to system instabilities[7]. The undesirable interaction of the controller with the ignored modes is often referred to as "spillover" effect.

Considerable attention has been devoted to the design of reduced order controllers[9,10]. However, very little work has been done in the area of choosing actuator/sensor placements. Yet this is a fundamental constraint of the control problem. Essentially, our ability to control a flexible system can only be as good as our actuator/sensor placement allows. For example, if actuators and sensors are located only on zero deflection points of a mode shape, that mode cannot be controlled. This study undertakes the development of a methodology for actuator and sensor placement to allow vibrational control of the system.

1.2 Current Methods for Actuator/Sensor Placement

It is generally recognized that the actuator placement problem and the sensor placement problem are dual problems[11]. This study focuses on the actuator placement issue only. Current methods for actuator placement range from intuitive placement to quite complex procedures based on controllability assessment schemes. Although intuitive schemes seem to work quite well for simple structures (e.g. beam, plate) they deteriorate as the complexity of the structure and the order of the model increase. For example, in a free-free beam modeled with the first two vibrational modes it is clear that we want to locate actuators near the peaks of the mode shapes for the best control authority over the system. However, as the order of the model is increased, it is unclear which locations should be chosen since each mode will have a different effect on the system performance and there are multiple peaks in each mode shape.

There have been several attempts to determine optimal actuator placement using controllability criteria[12-15]. Vander Velde has even extended the concept to include reliability and redundancy issues[15]. The basic philosophy of these schemes is to define a measure of the degree of controllability and use it to evaluate alternative placements of actuators. The objective is to find a set of actuators with the maximum degree of controllability. Unfortunately, these methods tend to be computationally intensive and thus are not applicable for high order systems. The reason for these computational difficulties is two fold. First, the degree of controllability is calculated via a controllability grammian, a non-trivial procedure. Second, as the number of possible actuator locations is increased, the number of possible actuator sets that must be evaluated increases dramatically. Another problem with these methods is that they neglect to take spillover into account. Thus, a method for actuator placement more compatible with high order systems must be developed.

1.3 Goals of Study

What we hope to attain in the present effort is a simplified method for actuator placement for vibration control of LSS. Our purpose is to devise a scheme which overcomes the computational difficulties associated with high order systems. Ideally this method would choose actuator placements such that they have good control authority over the primary modes while taking spillover considerations into account.

1.4 Approach

It is possible to represent both actuators and linear system performance measures as vectors in modal coordinates. These vectors are termed node shapes and their elements are the modal displacements appropriate to the actuator or the performance measure. The actuator selection problem becomes that of a choice of a set of actuator node shapes such that they form a good match to the performance node shape. This idea can be stated mathematically as

$$\underline{f}_* \doteq \bar{F} \cdot \underline{\alpha}$$

where

$\underline{f}_*$ is the performance node shape

$\doteq$ means "approximately equal"

$\bar{F}$ is a matrix of actuator node shapes

$\underline{\alpha}$ is some arbitrary vector of appropriate dimension

If there is an initial set of N actuator node shapes (corresponding to N possible actuator locations) equation (1-1) can be formulated as the following optimization problem

$$\min_{\underline{\alpha}, m_u} \left[\underline{f}_* - \sum_{j=1}^{m_u} \alpha_j \underline{f}_j\right]^T \bar{D} \left[\underline{f}_* - \sum_{j=1}^{m_u} \alpha_j \underline{f}_j\right] \tag{1-2}$$

i.e. find the set of m_u actuator node shapes which best approximate $\underline{f}_*$ in the least squares sense. The $\bar{D}$ matrix is to weight the modes according to their contribution to performance. To our knowledge the above problem has not been solved. Thus, two procedures are suggested to obtain an acceptable (suboptimal) solution to the actuator placement problem.

In the first method the initial set of N actuators is reduced using a QR factorization technique to solve the least squares problem. The QR factorization as employed here can be used to select a set of independent actuators to control the system. In the second method, actuators are selected one by one, each actuator complimenting the already existing set. Actuators are chosen so as to increse the control authority of the actuator set while minimizing spillover.

1.5 Results

The above procedures are used to place actuators on a cantilever beam. Both procedures result in actuator placement that match the intuitive concept of placing actuators near peaks of mode shapes. The effect of the actuator placement on the performance and stability of an LQG based controller is also demonstrated.

1.6 Organization of Thesis

The remainder of the thesis is divided into seven chapters. Chapter 2 discusses finite element models and the node shape concept. Chapter 3 discusses reduced order controllers. Chapter 4 presents the actuator selection problem and Chapter 5 presents two methods for actuator selection. Chapter 6 discusses the application of the selection procedures to an example structure. Chapter 7 contains concluding remarks.

CHAPTER 2

SYSTEM REPRESENTATION

2.1 Coordinate Transformation

Large space structures are lightweight, flexible and lightly damped. They are essentially distributed parameter systems that should be represented by partial differential equations. A convenient model for structures is obtained via an infinite number of modes of vibration plus the rigid body modes. In practice, it is sufficient to analyze these structures retaining a finite number of modes obtained via the finite element method. Computer packages such as NASTRAN are commonly used for this purpose[16].

In finite element analysis, the structure is modeled as a large number of elements connected at nodes[1]. The mass of the structure is considered to be lumped at the nodes and the connecting elements are modeled as perfect springs and dampers. This representation is often transformed from physical to modal (or normal) coordinates. This allows structural dynamics to be viewed as a set of uncoupled modal motions. Since low frequency modes will dominate the motion of the structure, it is reasonable to approximate the structure by eliminating the high frequency modes from the model.

The "physical" system equations of motion obtained via the finite element method with N nodes is given by

---

1 In finite element analysis a node is defined as a grid point on the structure, not necessarily a point where the modal deflection is zero.

$$\bar{M}\ddot{\underline{q}} + \bar{D}\dot{\underline{q}} + \bar{K}\underline{q} = \underline{h} \tag{2-1}$$

where

$\underline{q}$ is a 6N vector of generalized displacements (i.e. each node has 6 degrees of freedom, 3 translational and 3 rotational)

$\underline{h}$ is a vector of generalized external forces

$\bar{M}$ is a real , symmetric, positive definite mass matrix

$\bar{D}$ is a real matrix of inherent structural damping

$\bar{K}$ is a real, symmetric, positive semi-definite stiffness

The system equation (2-1) is conveniently transformed into modal coordinates via the transformation

$$\underline{q} = \bar{\Phi}\,\underline{\eta} \tag{2-2}$$

where

$\bar{\Phi}$ is the matrix mode shapes orthonormalized with respect to the mass matrix as in equation (2-4). (See discussion in the following section).

$\underline{\eta}$ is the vector of modal coordinates (amplitudes)

If M modes are retained in the finite element model then $\bar{\Phi}$ is of dimension 6N×M and $\underline{\eta}$ is of length M. Substituting equation (2-2) into equation (2-1) yields

$$\bar{M}\bar{\Phi}\ddot{\underline{\eta}} + \bar{D}\bar{\Phi}\dot{\underline{\eta}} + \bar{K}\bar{\Phi}\underline{\eta} = \underline{h} \tag{2-3}$$

where $\bar{\Phi}$ is chosen such that

$$\bar{\Phi}^T\bar{M}\bar{\Phi} = \bar{I} \tag{2-4}$$

$$\bar{\Phi}^T\bar{K}\bar{\Phi} = \bar{\Omega}^2 \tag{2-5}$$

At this step $\bar{D}$ is defined so that it satisfies

$$\bar{\Phi}^T\bar{D}\bar{\Phi} = 2\bar{Z}\bar{\Omega} \tag{2-6}$$

where $\bar{Z}$ is a diagonal matrix of damping ratios (chosen arbitrarily). The vector of generalized forces can be written as

$$\underline{h} = \bar{B}_u\underline{u} + \bar{B}_d\underline{d} \tag{2-7}$$

Thus, the system equation in modal coordinates is given by

$$\underline{\ddot{\eta}} + 2\bar{Z}\bar{\Omega}\underline{\dot{\eta}} + \bar{\Omega}^2\underline{\eta} = \bar{\Phi}^T\bar{B}_u\underline{u} + \bar{\Phi}^T\bar{B}_d\underline{d} \tag{2-8}$$

where

$\bar{Z}$ = $\mathrm{DIAG}(\zeta_1, \cdots, \zeta_m)$

$\bar{\Omega}$ = $\mathrm{DIAG}(\omega_1, \cdots, \omega_m)$

$\bar{\Phi}$ = $[\underline{\phi}_1, \cdots, \underline{\phi}_m]$

$\underline{\phi}_i$ is the mode shape vector of the ith mode of vibration

ζ_i is the damping ratio of the ith mode

ω_i is the natural frequency of the ith mode

$\underline{u}$ = $(u_1, \cdots, u_{m_u})$ the control inputs from m_u actuators

$\underline{d}$ = $(d_1, \cdots, d_{m_d})$ the disturbance inputs from m_d disturbance sources

$\bar{B}_u$ and $\bar{B}_d$ are selection matrices (see following section).

2.2 The Modal and Selection Matrices

2.2.1 Mode Shape

As stated in the last section, the modal matrix $\bar{\Phi}$ is the matrix of mode shapes orthonormalized with respect to the mass matrix.

Definition 1 - The ith mode shape ϕ_i is the vector of the displacements of the N nodes due to a unit amplitude of the ith mode.

Since there are six degrees of freedom for each node, the mode shape vector is of dimension 6N where the first N elements correspond to displacements in the first degree of freedom.

2.2.2 Selection Matrix

Equation (2-2) can be used to find the physical displacements in 6 degrees of freedom given the modal coordinate vector $\underline{\eta}$. Consider the motion of a single node in one of its degrees of freedom, x. This can be written

$$x = \underline{b}^T \bar{\Phi} \underline{\eta} \tag{2-9}$$

where $\underline{b}$ is a 6N boolean selection vector with one non-zero element that specifies the node and degree of freedom of interest. If we generalize x to a vector of j displacements, we can form the selection matrix -

$B = [\underline{b}_1, \cdots, \underline{b}_j]$ to obtain

$$\underline{x} = \bar{B}^T \bar{\Phi} \underline{\eta} \tag{2-10}$$

2.2.3 Node Shape

In analogy to the concept of the mode shape, it is convenient to describe the modal displacements of a single node in a specified degree of freedom. Thus, define the product $\bar{\Phi}^T \underline{b}$ as the node shape vector, $\underline{f}$, associated with $\underline{b}$.

Definition 2 - A node shape is a vector of length M, the entries of which are the displacements of a node due to each mode excited to a unit amplitude.

Thus the nodal displacement in the specified degree of freedom can be written

$$x = \underline{f}^T \underline{\eta}$$

The product $\bar{\Phi}^T \bar{B}$ is defined as the *node shape matrix*, $\bar{F}$.

The node shape is a versatile concept when $\underline{b}$ is not restricted to be a boolean selection vector. We demonstrate below how node shapes can be used to define quantities such as translation or rotation in an arbitrary direction, axial displacement between nodes, and the performance of the system.

2.2.2.1 Translation node shape

Consider the translation of a node in the direction of a unit vector $\underline{r} = (r_1, r_2, r_3, 0, 0, 0)$. The physical translational displacement vector of a node is given by $\underline{x} = (x_1, x_2, x_3, 0, 0, 0)$, so the displacement in the direction $\underline{r}$ is

$$x_r = \frac{\underline{x} \cdot \underline{r}}{\underline{r} \cdot \underline{r}} |\underline{r}| = \underline{x} \cdot \underline{r} \tag{2-11}$$

To form the dot product for the ith node in modal coordinates we specify the selection vector $\underline{b}$ via its entries b_k as follows

$$b_k = \begin{cases} r_1 & \text{when } k = i \\ r_2 & k = N + \ell \\ r_3 & k = 2N + i \\ 0 & \text{OTHERWISE} \end{cases}$$

The resulting node shape is

$$\underline{f} = \bar{\Phi}^T \underline{b}$$

It can be used to find the translation in the direction $\underline{r}$ as

$$x_r = \underline{f}^T \underline{n} \tag{2-12}$$

Thus, the node shape could be used to represent a position sensor or a force actuator oriented in the direction $\underline{r}$. This is trivially extended to represent a rotation vector in a specified direction at a selected node.

2.2.2.2 Axial node shape

The axial node shape is representative f the axial elongation of a member connecting two nodes. If the member is much longer than the expected elongation, it is, approximately correct to write

$$x_{12} \simeq \underline{x}_2 \cdot \underline{r} - \underline{x}_1 \cdot \underline{r} \tag{2-13}$$

where

x_{12} is the elongation or contraction of the element connecting nodes 1 and 2

$\underline{x}_1$ and $\underline{x}_2$ are the translational displacement vectors at nodes 1 and 2

$\underline{r}$ is a unit vector directed at node 2 from node 1

Using Equations (2-11) and (2-12), Equation (2-12) can be written as

$$x_{12} \simeq (\underline{f}_2 - \underline{f}_1)^T \underline{n}$$

which shows the axial node shape, $\underline{f}_{12}$, as given by the difference between the two translational node shapes in the direction of the connecting element, i.e.

$$\underline{f}_{12} = \underline{f}_2 - \underline{f}_1$$

to give the axial elongation

$$x_{12} = \underline{f}_{12}^T \underline{n}$$

2.2.2.3 Performance node shape

The performance of a system is frequently given by some linear combination of the translations and rotations of some nodes on the structure. A typical example is the line of sight (LOS) error for optical systems. Although not in strict accordance with definition 2, we can form a node shape that represents system performance. Considering the performance measure y

$$y = a_1 x_1 + a_2 x_2 + \cdots + \alpha_n x_n \qquad (2\text{-}14)$$

where

$a_1 - a_n$ are constant coefficients

$x_1 - x_n$ are translational or rotational deflection of nodes

Equation (2-14) can be rewritten as

$$y = a_1\underline{f}_1^T\underline{n} + a_2\underline{f}_2^T\underline{n} + \cdots + a_n\underline{f}_n^T\underline{n}$$

Defining the vector $\underline{a}$ as

$$\underline{a} = (a_1, a_2, \cdots, a_n)$$

and recalling that

$$\underline{f}_1 = \bar{\Phi}^T\underline{b}_1$$

$$\bar{B} = [\underline{b}_1, \underline{b}_2, \cdots, \underline{b}_n]$$

The performance node shape $\underline{f}_*$ can be defined as

$$\underline{f}_* = \bar{\Phi}^T\bar{B}\underline{a}$$

so that the performance measure is given by

$$y = \underline{f}_*^T\underline{n}$$

CHAPTER 3

LARGE SPACE STRUCTURE CONTROLLERS

3.1 Introduction

As noted in Chapter 2, finite element methods can be used to approximate a system of infinite order using only M modes. Unfortunately the dimension of the system is still too large to allow construction of a practical full state feedback controller. This is due to onboard computer limitations and the difficulty in computing optimal control gains for high order systems[5]. A common approach to the control design is to identify a set of primary modes, usually based on system performance, and design a controller based on those modes only[7,8]. The goal is the control of the full order system with this reduced order controller.

3.2 State Equation Development

The system equation is given in Equation (2-8) as

$$\ddot{\underline{\eta}} + 2\bar{Z}\bar{\Omega}\dot{\underline{\eta}} + \bar{\Omega}^2\underline{\eta} = \bar{\Phi}^T\bar{B}_u\underline{u} + \bar{\Phi}^T\bar{B}_d\underline{d}$$

In addition, the measurement equations can be written as

$$\underline{y}_x = \bar{B}_x^T\Phi\underline{\eta} + \underline{v}_x \qquad (3\text{-}1)$$

$$\underline{y}_v = \bar{B}_v^T \Phi \dot{\underline{n}} + \underline{v}_v \tag{3-2}$$

where

$\underline{y}_x$ is a vector of position sensor output

$\underline{y}_v$ is a vector of velocity sensor output

$\bar{B}_x$ and $\bar{B}_v$ are the appropriate selection matrices

$\underline{v}_x$ and $\underline{v}_v$ represent sensor noise

The corresponding state equation is

$$\dot{\underline{x}} = \bar{A}\underline{x} + \bar{B}\underline{u} + \bar{\Gamma}\underline{d} \tag{3-3}$$

$$\underline{y} = \bar{C}\underline{x} + \underline{v} \tag{3-4}$$

For the representation in (2-8), (3-1) and (3-2), the various entries of (3-3) and (3-4) are defined as follows:

$$\bar{A} = \left[\begin{array}{c|c} 0 & I \\ \hline -\bar{\Omega}^2 & -2\bar{Z}\bar{\Omega} \end{array}\right] \qquad \bar{B} = \left[\begin{array}{c} 0 \\ \hline \Phi^T\bar{B}_u \end{array}\right]$$

$$\bar{\Gamma} = \left[\begin{array}{c} 0 \\ \hline \bar{\Phi}^T B_d \end{array}\right] \qquad \underline{x} = \begin{bmatrix} \underline{n} \\ \dot{\underline{n}} \end{bmatrix} \tag{3-5}$$

$$\underline{y} = \begin{bmatrix} \underline{y}_x \\ \underline{y}_v \end{bmatrix} \qquad C = \left[\begin{array}{c|c} \bar{B}_x^T\Phi & 0 \\ \hline 0 & \bar{B}_v^T\Phi \end{array}\right]$$

$$\underline{v} = \begin{bmatrix} \underline{v}_x \\ \underline{v}_v \end{bmatrix}$$

By selecting L primary modes, equations (2-8), (3-1), and (3-2) can be represented via primary and residual components.

$$\underline{\ddot{\eta}}_P + 2\bar{Z}_P\bar{\Omega}_P\underline{\dot{\eta}}_P + \bar{\Omega}_P^2\underline{\eta}_P = \bar{\Phi}_P^T\bar{B}_{uP}\underline{u} + \bar{\Phi}_P^T\bar{B}_{dP}\underline{d}$$

$$\underline{\ddot{\eta}}_R + 2\bar{Z}_R\bar{\Omega}_R\underline{\dot{\eta}}_R + \bar{\Omega}_R^2\underline{\eta}_R = \bar{\Phi}_R^T\bar{B}_{uR}\underline{u} + \bar{\Phi}_R^T\bar{B}_{dR}\underline{d}$$

$$\underline{y}_x = \bar{B}_{xP}^T\bar{\Phi}_P\underline{\eta}_P + \bar{B}_{xR}^T\bar{\Phi}_R\underline{\eta}_R + \underline{v}_x$$

$$\underline{y}_v = \bar{B}_{vP}^T\bar{\Phi}_P\underline{\dot{\eta}}_P + \bar{B}_{vR}^T\bar{\Phi}_R\underline{\dot{\eta}}_R + \underline{v}_v$$

where subscript P is associated with primary modes and subscript R with residual modes.

Equations (3-6) are written in state equation form as

$$\begin{bmatrix} \underline{\dot{x}}_P \\ \underline{\dot{x}}_R \end{bmatrix} = \begin{bmatrix} \bar{A}_P & 0 \\ 0 & \bar{A}_R \end{bmatrix} \begin{bmatrix} \underline{x}_P \\ \underline{x}_R \end{bmatrix} + \begin{bmatrix} \bar{B}_P \\ \bar{B}_R \end{bmatrix} \underline{u} + \begin{bmatrix} \bar{\Gamma}_P \\ \Gamma_R \end{bmatrix} \underline{d} \qquad (3\text{-}7)$$

$$\underline{y} = [\bar{C}_P \quad \bar{C}_R] \begin{bmatrix} \underline{x}_P \\ \underline{x}_R \end{bmatrix} + \underline{v}$$

3.3 Controller Design

The reduced order controller is designed based on the primary modes only. Restricting attention to optimal (modern) control philosophy, the controller is comprised of two parts:

1) A state estimator which accepts the sensor measurements $\underline{y}$ and produces an estiamte $\underline{\hat{x}}_P$ of the primary states $\underline{x}_P$

2) A linear state feedback control law which multiplies the state estimate $\underline{\hat{x}}_P$ by a constant gain matrix to produce the actuator commands $\underline{u}$.

The state estimator equation is

$$\dot{\hat{\underline{x}}}_p = \bar{A}_p\hat{\underline{x}}_p + \bar{B}_p\underline{u} + \bar{G}\left(\underline{y} - \bar{C}_p\hat{\underline{x}}_p\right) \tag{3-8}$$

where $\bar{G}$ is the constant estimator gain matrix. The control law is given by

$$\underline{u} = \bar{K}\hat{\underline{x}}_p \tag{3-9}$$

where $\bar{K}$ is the constant feedback gain matrix. Using equations (3-7) and (3-9) we can rewrite (3-8) as

$$\dot{\hat{\underline{x}}}_p = \left(\bar{A}_p + \bar{B}_p\bar{K} - \bar{G}\bar{C}_p\right)\hat{\underline{x}}_p + \bar{G}\bar{C}_p\underline{x}_p + \bar{G}\bar{C}_R\underline{x}_R + \bar{G}\underline{v} \tag{3-10}$$

Defining the estimate error, $\underline{e}$ as

$$\underline{e} \equiv \underline{x}_p - \hat{\underline{x}}_p$$

The estimate error equation can be written as

$$\dot{\underline{e}} = \left(\bar{A}_p - \bar{G}\bar{C}_p\right)\underline{e} - \bar{G}\bar{C}_R\underline{x}_R$$

So the total system state equations can be written as

$$
\begin{bmatrix} \dot{\underline{x}}_p \\ \dot{\underline{e}} \\ \dot{\underline{x}}_R \end{bmatrix} = \begin{bmatrix} \bar{A}_p + \bar{B}_p K & -\bar{B}_p \bar{K} & 0 \\ 0 & \bar{A}_p - \bar{G}\bar{C}_p & -\bar{G}\bar{C}_R \\ \bar{B}_R \bar{K} & -\bar{B}_R \bar{K} & \bar{A}_R \end{bmatrix} \begin{bmatrix} \underline{x}_p \\ \underline{e} \\ \underline{x}_R \end{bmatrix} + \begin{bmatrix} \bar{\Gamma}_p \\ \bar{\Gamma}_p \\ \bar{\Gamma}_R \end{bmatrix} \underline{d} + \begin{bmatrix} 0 \\ -G \\ 0 \end{bmatrix} \underline{v} \quad (3\text{-}11)
$$

Block diagrams of the controller and the controlled system are given in Figures (3-1) and (3-2).

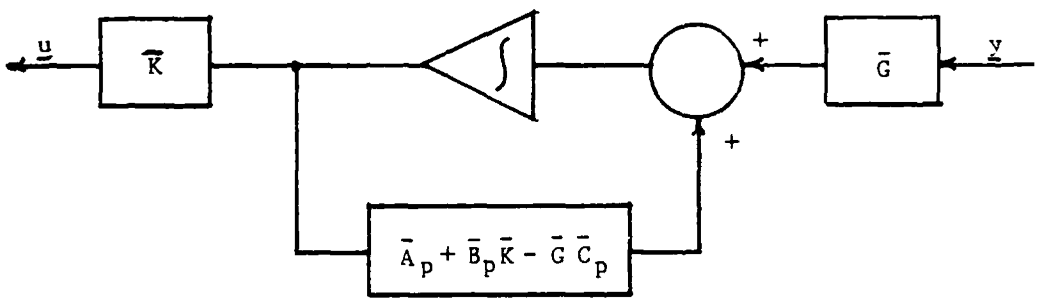

Figure 3-1 Feedback Controller

The selection of the gain matrices $\bar{K}$ and $\bar{G}$ is a standard procedure given the correct plant model[17]. However, the task is complicated due to the reduced order model used in the controller design, which in turn leads to spillover effect (discussed in next section). The proper selection of gain matrices to accommodate spillover is beyond the scope of this study and will not be discussed (see [9-10] for some possible solutions).

3.4 Spillover

One of the major problems to be considered in reduced order controller design is spillover. Spillover is the adverse interaction of the controller with the residual modes. Considering Figure 3-2, the residual modes are excited by

$$\bar{B}_R \underline{u} = \bar{B}_R \bar{K} \hat{\underline{x}}_P$$

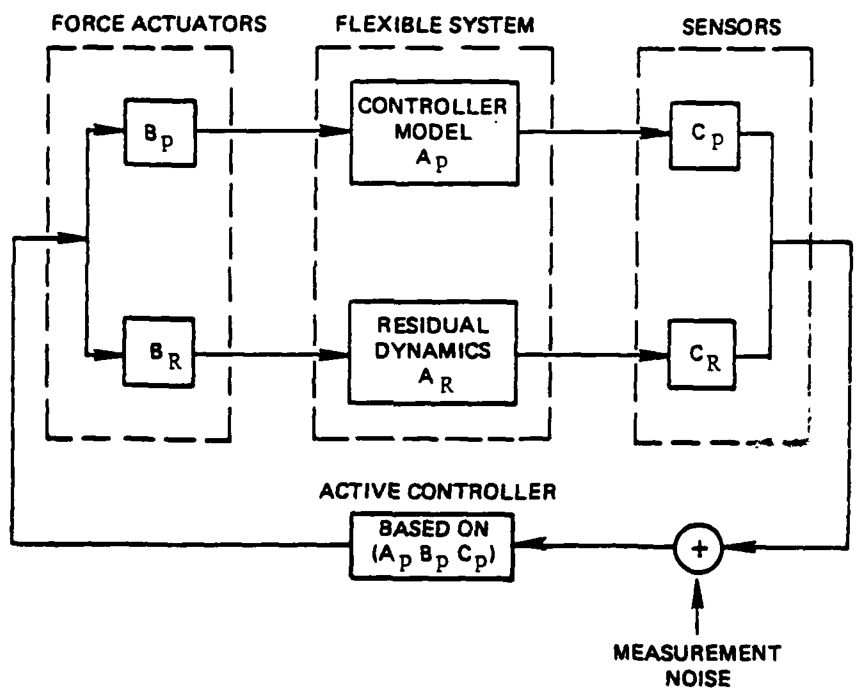

Figure 3-2 System with Reduced Order Controller

This is called control spillover. Furthermore, the measurements, y are contaminated by the term $\bar{C}_R x_R$. This in turn lead to errors in the

estimate $\hat{\underline{x}}_P$. The contamination of sensor readings by residual modes is termed observation spillover.

Control spillover alone is probably not a major problem. If there is no observation spillover (i.e. $\bar{C}_R = 0$), then from equations (3-11) the eigenvalues of the controlled system can be obtained from $(\bar{A}_P+\bar{B}_P\bar{K})$, $(\bar{A}_P-\bar{G}\bar{C}_P)$, and $\bar{A}_R$. Assuming the residual modes are open loop stable (even if only marginally stable) and that the regulator and observer are stable, the only effect of control spillover is to excite the residual modes. This will tend to deteriorate performance, but will not lead to instability.

However, observation spillover might lead to instabilty[7]. Considering Equation (3-11), if $\bar{C}_R \neq 0$ then the system eigenvalues will be dependent on $\bar{C}_R$. Thus the closed loop poles might migrate to the right half s-plane, especially considering the low damping of the structure.

CHAPTER 4

ACTUATOR PLACEMENT PROBLEM

4.1 Introduction

Actuator locations are a fundamental constraint of the LSS controller design problem. It is desirable to place actuators such that:

1) control authority over the L primary modes is maximized
2) spillover to residual modes is minimized
3) a small number of actuators is used
4) the actuator set is balanced, namely that actuators are operating at comparable/acceptable power levels

The actuator placement problem is usually subject to the following constraints

1) actuator type
2) physical limitations on actuator location

In this chapter the constraints and placement criteria are discussed in detail, then a mathematical formulation of the actuator placement problem is presented.

4.2 Constraints

4.2.1 Actuator Type

In most design applications, the choice of actuator type is constrained. This might be due to problems with contamination by propellants, power supply limitations, cost, etc. An important consideration in selecting actuators for LSS applications is the

availability of broad band (especially low frequency) actuators. Another desirable actuator characteristic is its operation with no interaction with the rigid body modes. Thus propellant devices and momentum wheels are of limited use in vibration control. Member actuators are desirable due to their lack of effect on the rigid body motion and their spectral characteristics.

4.2.2 Physical Limitations

There are locations on a structure where the placement of actuators is forbidden. These forbidden regions are usually due to 1) the sensitivity of nearby equipment or 2) portions of the structure being too weak to withstand actuator inputs of the magnitude required. In the first case, effects like the outgassing of propellant actuators must be considered. In the second case, locations such as mirror mounts are usually forbidden.

4.3 Criteria for Placement

4.3.1 Control Authority

Actuator placement to maximize the control authority over the primary modes means selecting actuator locations such that the actuators are operating at the minimum possible power levels to meet performance specifications. For example, consider a single mode shape. It is clear that locating an actuator at the peak of the mode shape will give better control authority over that mode than an actuator located off the peak. Thus, actuator node shapes that provide good control authority should have large elements corresponding to the primary modes.

4.3.2 Spillover

It is desirable to place actuators such that excitation of the residual modes is minimal. This in turn would result in better control when the reduced order controller is applied to the structure. There are

two considerations when choosing actuator locations to minimize spillover. First, actuators should be located as close to the zero deflection points of the residual mode shapes as possible. In general, this is not possible for all of the residual modes. A possible solution is to choose a subset of the most critical residual modes, termed secondary modes, and choose actuator locations near their zero deflection points (i.e. small entries in the actuator node shapes corresponding to residual modes). The second consideration is the applied actuation force. If an actuator is moved away from a point where it has good control authority, it will require larger actuation forces to control the system. In general, larger actuation forces imply more spillover to the residual modes. Thus, there is a tradeoff to be considered in choosing actuator locations for spillover prevention.

4.3.3 Number of Actuators

Choosing the optimum number of actuators to control the system is not a trivial problem. For economic considerations, the number of actuators should be kept small. However, if redundancy is a major consideration, the actuator set should be larger than the minimum required to maintain control. For the purposes of this study, redundancy issues are ignored and the smallest set that retains good control authority is sought.

A system is said to be controllable if it can be transferred from any initial state $\underline{x}(0)$ to a final state $\underline{x}(t_f)$ in finite time by some control $\underline{u}$. Thus, controllability is the ability of the control input to affect each state variable. Now, consider a LSS with L primary modes. The above implies that a single actuator can control the primary modes if all the corresponding elements in the actuator node shape are non-zero (note, this is true as long as each mode has different frequencies). On the other hand, L actuators can be found such that practically each mode is independently controlled by a single actuator.

Unfortunately controllability is simply a binary concept - either a system is controlled or it is not. It is intuitively obvious that increasing the number of actuators will increase the control authority of the actuator set, just as increasing the number of measurements will increase the accuracy of an estimte produced by an estimator. However, if initial actuator locations are well selected, diminishing returns are expected as the number of actuators approaches L[2]. If actuators are placed such that individual actuators have good control authority over several modes, then it is possible that less than L actuators will provide approximately the same control authority over the primary modes as L actuators.

4.3.4 Balanced Set

It is desirable to have the actuators working at comparable power levels. This is convenient since identical actuators can be used throughout the structure which simplifies the design procedure and reduces cost.

4.4 Mathematical Formulation

Expressing the above objectives in a mathematical expression which is ameanable to actuator placement procedures is difficult if not impossible. In the following, some possible engineering solutions which approach the goals stated above are presented.

In Chapter 2, the concept of the node shape is developed. It is demonstrated that node shapes can be created to represent actuator influence and system performance measures. Thus, the problem of actuator placement can be mathematically stated as that of choosing a set of actuator node shapes such that a linear combination of them is approximately equal to the performance node shape [18], i.e.

$$\underline{f}_{*} \doteq \bar{F} \cdot \underline{\alpha} \qquad (4\text{-}1)$$

where

$\underline{f}_*$ is the performance node shape

$\doteq$ means "approximately equal"

$\bar{F}$ is a matrix of actuator node shapes

$\underline{\alpha}$ is some arbitrary vector of approximate dimension

The above formulation can be somewhat simplified if an initial set of n possible actuator locations has already been selected. This initial set is selected subject to constraints on actuator type and location. The problem then reduces to a selection of m_u node shapes from the initial set which provide a good approximation of $\underline{f}_*$. This selection is subject to the criteria:

1) Maximize control authority: The match to the performance node shape is good, entries in $\bar{F}$ corresponding to primary modes are large, $\underline{\alpha}$ components are small

2) Minimize spillover: The entries in $\bar{F}$ corresponding to secondary modes are small.

3) Small actuator set: m_u is small

4) Balance: All the $\underline{\alpha}$ components are of comparable magnitude

In the following section, the quadratic cost function is proposed as the mathematical criterion for "approximately equal".

4.4.1 Least Squares Formulation

The selection criteria can be formulated as

$$|\underline{r}|^2 = [\underline{f}_* - \sum_{i=1}^{m_u} \underline{f}_i \alpha_i]^T \bar{D}[\underline{f}_* - \sum_{i=1}^{m_u} \underline{f}_i \underline{\alpha}_i] \qquad (4-2)$$

where m_u and $\underline{\alpha}$ are chosen to minimize the squared magnitude of the residual vector $\underline{r}$. The purpose of the diagonal matrix $\bar{D}$ is to weight the different modes according to their importance to the control ··oblem. In effect, the $\bar{D}$ matrix reduces the order of the problem to con..der only the primary modes. Thus, L non-zero values and m-L zero values are expected among the elements of $\bar{D}$. A possible selection for $\bar{D}$ is to use ones for the elements corresponding to residual modes. However, this does not reflect relative importance among the primary modes. Thus, the elements of $\bar{D}$ corresponding to primary modes should reflect the contribution of each mode to overall performance.

For example, for a given disturbance acting on the system, a set of mean square modal amplitudes, $\underline{\eta}_{ms}$, can be obtained. If the intra mode interaction is small, it is reasonable to approximate the contribution of the ith mode to the mean square performance as $\left(f_*\right)_i^2\left(\eta_{ms}\right)_i$. Thus the $\bar{D}$ matrix could be defined as

$$\bar{D} = \text{diag}\left((f_*)_i^2\right) \text{diag}\left((\eta_{ms})_i\right) \text{diag}\,(w_i)$$

where

i ranges from 1 to M

$w_i = 1$ for primary modes

$w_i = 0$ for residual modes

CHAPTER 5

ACTUATOR SELECTION PROCEDURES

5.1 General Method

In Chapter 4 a set of constraints and criteria were developed for the actuator placement problem. The placement problem was then mathematically formulated as a least squares problem. To our knowledge, the least squares problem as presented has not been solved, thus a suboptimal approach is taken to solve the least squares problem. The suggested general procedure consists of the following major steps:

1) Define a large initial set
2) Choose L actuators to solve the least squares problem
3) Reduce the set of L actuators if possible
4) Augment the initial set if necessary

A flow chart of the general procedure is given in Figure 5-1. Each of the above steps is discussed in detail in the following sections.

5.2 Initial Set

The initial set of actuator locations is ideally an infinite set containing all permissable actuator locations. This obviously being impossible, a large set that is representative of the infinite set is selected. The first constraint that must be considered is what type (or types) of actuators can be used to control the structure. As noted in Chapter 4, it is desirable to use member actuators since they do not affect rigid body modes. Thus, whenever possible, member actuators should be used in the formulation of the initial set. Actuators of the type(s) chosen are placed at a large number of locations on the

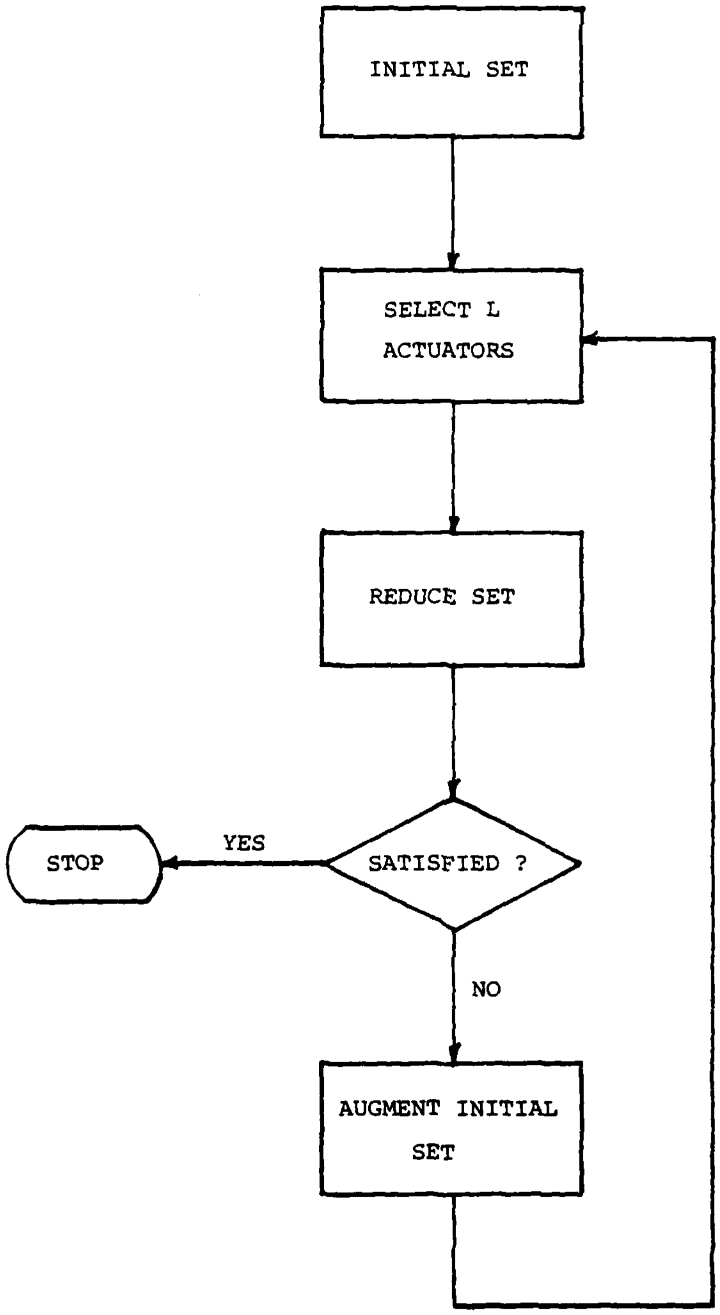

Figure 5-1 General Actuator Selection Procedure

structure, avoiding those areas where actuator placement is physically prohibited.

For example, if only axial actuator are to be used to control a truss structure, a simple initial set would be the placement of an actuator on each member.

5.3 Least Squares Solution Based on L Actuators

The solution of the least squares problem presented in Chapter 4 involves the selection of m_u actuators and the components of $\underline{\alpha}$ to minimize the norm of the least squares residual vector. As a first step in the suboptimal solution, L actuators are chosen from the initial set and the components of $\underline{\alpha}$ calculated. In this section a numerical technique to solve for the $\underline{\alpha}$ components and two methods for selecting L actuators from the initial set are presented.

Before continuing with this section, some new notation is required that willbe used throughout the chapter. The least squares formulation presented in Chapter 4 was reduced to consideration of weighted primary modes. Thus, the quantities of interest can be represented as

$$\begin{bmatrix} f_w \\ -- \\ 0 \end{bmatrix} = \left(\bar{D}\right)^{\frac{1}{2}} \underline{f}$$

$$\begin{bmatrix} \bar{F}_w \\ -- \\ 0 \end{bmatrix} = \left(\bar{D}\right)^{\frac{1}{2}} \bar{F}$$

$$\begin{bmatrix} \underline{f}_{*w} \\ --- \\ 0 \end{bmatrix} = \left(\bar{D}\right)^{\frac{1}{2}} \underline{f}_{*}$$

$$\begin{bmatrix} \underline{r}_w \\ -- \\ 0 \end{bmatrix} = \underline{r}$$

where it is assumed that the primary modes have been pivoted to the top of the appropriate vectors. Thus Equation (4-2) is rewritten

$$|r_w|^2 = [\underline{f}_{*w} - \sum_{i=1}^{m_u} \underline{f}_{wi}\alpha_i]^T [\underline{f}_{*w} - \sum_{i=1}^{m_u} \underline{f}_{wi}\alpha_i]$$

5.3.1 QR Factorization

The QR factorization is a technique commonly used to obtain the $\underline{\alpha}$ components in a least squares problem. The concept is presented in the context of node shapes, but it can be generalized to any set of vectors. Let $\bar{F}_w$ be an L X m_u node shape matrix. Assume that $L \geq m_u$ and rank $(\bar{F}_w) = m_u$. There exists an orthogonal matrix $\bar{Q}$ such that $\bar{Q}^T\bar{F}_w$ is zero below its diagonal. Thus, $\bar{Q}^T\bar{F}_w$ can be written in the form

$$\bar{Q}^T\bar{F}_w = \begin{bmatrix} \bar{R} \\ - \\ 0 \end{bmatrix} \tag{5-1}$$

where $\bar{R}$ is a $m_u x m_u$ upper triangular matrix. In the case when $m_u = L$, Equation (5-1) is written

$$\bar{Q}^T\bar{F}_w = \bar{R}$$

which implies

$$\bar{F}_w = \bar{Q}\bar{R} \tag{5-2}$$

However, in the case where $m_u < L$, $\bar{Q}$ can be partitioned as

$$\bar{Q} = [\bar{Q}_1, \bar{Q}_2]$$

where $\bar{Q}_1$ is $L \times m_u$. Thus, $\bar{F}$ can be written as

$$\bar{F}_w = \bar{Q}_1 \bar{R} \tag{5-3}$$

Now, the least squares problem is

$$\bar{F}_w \underline{\alpha} \tilde{=} \underline{f}_{*w} \tag{5-4}$$

which can be rewritten as

$$\bar{Q}_1 R \underline{\alpha} \tilde{=} \underline{f}_{*w} \tag{5-5}$$

If $\bar{F}_w$ has linearly independent columns, as initially assumed, then $\bar{R}$ is nonsingular and

$$\underline{\alpha} = \bar{R}^{-1} \bar{Q}_1^T \underline{f}_{*w} \tag{5-6}$$

It can also be shown that the least squares residual vector, $\underline{r}_w$, is given by

$$\underline{r}_w = \bar{Q}_2 \bar{Q}_2^T \underline{f}_{*w}$$

(i.e. the projection of $\underline{f}_{*w}$ orthogonal to the span of $\bar{F}_w$). Thus, in the case m_u=L, $|r_w|$ = 0.

5.3.2 Maximum Norm Method

The QR factorization and least squares routines used in this study are standard LINPACK routines[21]. A pivoting option is included in the QR factorization routine that appears useful as a method to reduce the initial set to L actuators. Given an actuator node shape matrix for the initial set, $\bar{F}_{wI}$ of dimension Lxn where n is the number of actuators in the initial set, the pivoting routine selects a set of independent actuators from the initial set and pivots them to the front of $\bar{F}_{wI}$.

Conceptually, the pivoting procedure is as follows:

(1) Given $\bar{F}_{wI} = [\underline{f}_{w_1}, \cdots, \underline{f}_{w}]$, compute $||\underline{f}_w||$ for all n actuators (node shapes).

(2) Pivot node shape with maximum $||\underline{f}_w||$ to first column $\bar{F}_{wI}$

(3) Let i represent number of actuators already selected. For the n-i remaining node shapes, calculate the component orthogonal to the span of the i selected node shapes, $\underline{f}_w^{\perp}$

(4) Compute $||\underline{f}_w^{\perp}||$ for the n-i node shapes

(5) Pivot actuator with maximum $||\underline{f}_w^{\perp}||$ to the (i+1)th column of $\bar{F}_{wI}$

(6) If L node shapes have been selected, stop, otherwise return to step 3 and begin process to select another node shape.

The QR factorization procedure can now be performed on the first L columns of $\bar{F}_{wI}$. In practice, the pivoting and computation of the elements of $\bar{Q}$ and $\bar{R}$ takes place simultaneously[21]. They are separated here to make the presentation of the concepts clearer.

As a result of the pivoting option, the $\bar{R}$ matrix has diagonal elements, r_{ii}, which obey

$$|r_{11}| \geq |r_{22}| \geq \cdots \geq |r_{LL}|$$

where $|r_{ii}|$ is the norm of the component of $\underline{f}_{w_i}$ orthogonal to the span of $[\underline{f}_{w_1}, \underline{f}_{w_2}, \cdots, \underline{f}_{w_{i-1}}]$. If at some point $|r_{ii}| \approx 0$, there is not a set of L independent actuators in the initial set.

This pivoting routine appears useful for actuator selection for several reasons. First, maximum norm values are selected, which corresponds to the concept of attaining good control authority. Second, on independent set is selected, which corresponds to the concept of a small actuator set. Spillover and balance criteria have not been considered with this procedure.

5.3.3 Residual Matching Method

The second method for selecting L actuators from the initial set is conceptually similar to the maximum norm method. It is formulated to select an independent set of actuators that have good control authority over the primary modes and avoid spillover into selected secondary modes. This method is presented in the following two sections: in the first section control authority is considered and in the second section spillover is added to the formulation.

5.3.3.1 Control authority considerations

A diagram of the two vector least squares problem is given in Figure 5-2.

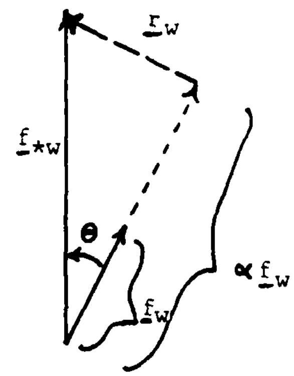

Figure 5-2 Two Vector Least Squares Problem

To obtain good control over the system with a single actuator, the angle θ between the performance node shape, $\underline{f}_{*w}$, and the actuator node shape, $\underline{f}_w$, should be small. In addition, to control with small actuation forces, the length of $\underline{f}_w$ should be large. Thus, a good measure of the control authority of a single actuator would be the length of the projection of the actuator node shape onto the performance node shape. This projection length can be written

$$\left| \frac{\underline{f}_w \cdot \underline{f}_{*w}}{\underline{f}_{*w} \cdot \underline{f}_{*w}} \underline{f}_{*w} \right|$$

Define a control authority ranking measure, c_i, for the ith actuator as

$$c_i = \left| \underline{f}_{w_i} \cdot \underline{f}_{*w} \right|$$

The above definition is adequate for non-vibrating systems, but must be modified for vibrational systems. The performance of vibratory systems is often measured in terms of mean square, or RMS, quantities. In node shape notation, the system performance is measured by

$$y = \underline{f}_*^T \underline{\eta}$$

The appropriate mean square measure is obtained from

$$E[y^2] = E[(\underline{f}_*^T \underline{\eta})^2] = E[(f_1 \eta_1 + \cdots + f_M \eta_M)^2]$$

If the intra-mode interaction is assumed small, it is approximately correct to write

$$E[y^2] \simeq f_{*_1}^2 E[\eta_1{}^2] + \cdots + f_{*_M}^2 E[\eta_M]^2$$

The purpose of the above is to demonstrate that the mean square performance is not significantly affected by the signs of the elements of $\underline{f}_*$ (i.e. they are always squared quantities). However, the control authority ranking measure developed above is highly dependent on the signs of the terms in $\underline{f}_*$. For example, if $\underline{f}_{*w}$ and $\underline{f}_w$ are given by

$$\underline{f}_{*w} = \begin{bmatrix} -1 \\ \\ 1 \end{bmatrix} \qquad \underline{f}_w = \begin{bmatrix} 1 \\ \\ 1 \end{bmatrix}$$

The ranking scalar, c_i, is equal to zero. This implies that $\underline{f}_w$ has no control authority over $\underline{f}_{*w}$. This is only true in the case where the two modes have the same frequency and are in phase. In general, this will not be true. Thus, the control authority ranking scalar must be

redefined so as to ignore the signs of the components of $\underline{f}_{*w}$. The ranking scalar is redefined such that the absolute value of each term in the dot product is used. Therefore

$$c_i = \sum_{j=1}^{L} \left| f_{w_j} f_{*w_j} \right|$$

With the above formulation, c_i should be a reasonable indication of the control authority of the ith actuator. Selection of the actuator with the largest c_i value would be a reasonable choice as the best actuator to control the system.

After selecting the first actuator to control the system, it is clear that if $\left|\underline{r}_w\right| \neq 0$ the match to the performance node shape can be improved by adding an actuator node shape in the direction $\underline{r}_w$. If the remaining actuators in the initial set are ranked by

$$c_i = \sum_{j=1}^{L} \left| f_{w_j} r_{w_j} \right|$$

the best actuator in the direction $\underline{r}_w$ can be selected. Each time an actuator is added to the set a new residual vector is calculated. The selection process continues until L actuators are selected. A flow chart of the procedure is given in Figure 5-3.

A property of the residual vector is that it is orthogonal to the space spanned by the actuator node shapes. Thus, an independent set of actuators is expected from this selection process. Thus the selected set should be an independent set with good control authority characteristics.

5.3.3.2 Spillover considerations

The residual mode equation present in Chapter 3 is

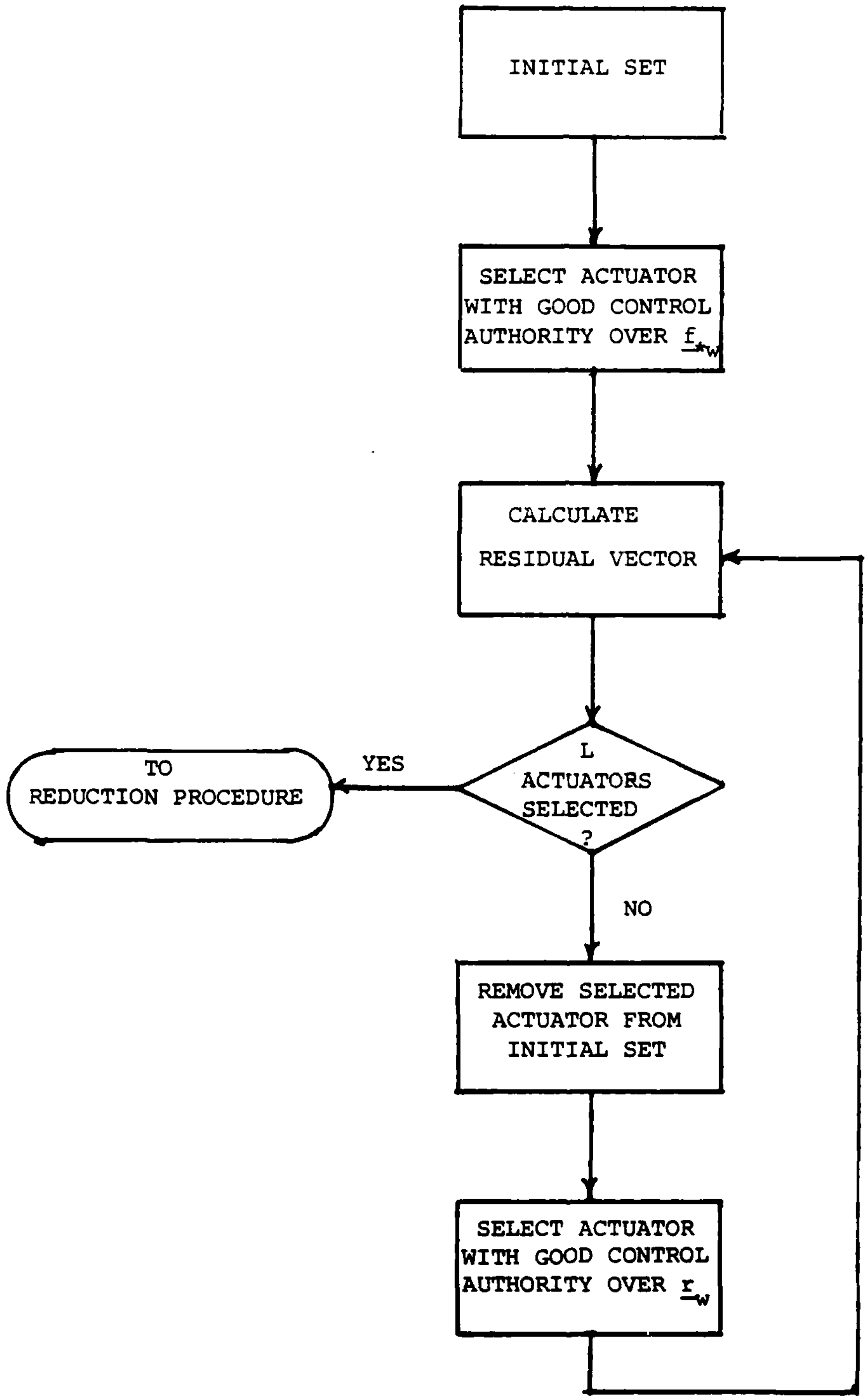

Figure 5-3 Residual Matching Procedure (Control Authority Only)

$$\ddot{\underline{\eta}}_R + 2\bar{Z}_R\bar{\Omega}_R\dot{\underline{\eta}}_R + \bar{\Omega}_R^2\underline{\eta}_R = \bar{\Phi}_R^T\bar{B}_{uR}\underline{u} + \bar{\Phi}_R^T\bar{B}_{dR}\underline{d}$$

The best spillover characteristics would be obtained if

$$\bar{B}_{uR} = 0$$

In general, the global prevention of spillover to residual modes via actuator placement is not possible. Thus, a reduced set of n_s modes is defined and actuator locations are selected to reduce spillover to those modes. The modes in this set are termed secondary modes. If $\bar{B}_{us}$ is defined as the rows of $\bar{B}_{uR}$ corresponding to secondary modes, then the actuator placement problem is defined in terms of minimizing $\bar{B}_{us}$.

Each column of $\bar{B}_{us}$ is the secondary mode elements, s_j, of an actuator node shape. Define a spillover ranking scalar, d_i, for the ith actuator in the initial set as

$$d_i = \frac{1}{\sqrt{\sum_{j=1}^{n_s} s_i^2}}$$

Thus, actuators with the smallest secondary mode elements can be chosen from the initial set. This spillover criteria can be combined with the control authority criteria developed above.

The suggested procedure is to first sort the initial set by control authority characteristics and then select a small set of the actuators with the best control authority. This set is then sorted by the spillover criteria and a single actuator chosen. In this manner a set of independent actuators with good control authority can be obtained while taking spillover into consideration.

The selection of the small set from the initial control authority ranking is as follows. Define c_{max} as the maximum control authority scalar obtained in the ranking procedure. If l is defined as a limiting factor, then those actuators with c_i values less than lc_{max} can be eliminated from the selection process. This reduced set can now be sorted by spillover characteristics. In working with several example structures (see Chapter 6), a value of l=0.9 appears to be a goodchoice. A flow chart of the modified selection procedure is given in Figure 5-4.

5.4 Reducing the Number of Actuators

A desirable set of actuators achieves good control authority and minimum spillover with a small set of actuators. In the above, a set of L actuator node shapes is chosen which results in a perfect match to the performance node shape (i.e. $|\underline{r}_w| = 0$). In this section a method is presented to identify which of the L actuators have the smallest contribution to the least squares fit. It is possible that these actuators can be removed from the set without causing a significant increase in $|\underline{r}_w|$ (i.e. $|\underline{r}_w| = 0$).

Equation 5-5 can be rewritten as

$$\underline{g} = \bar{R}\,\underline{\alpha} = \bar{Q}_1^T \underline{f}_{*w}$$

The columns of $\bar{Q}_1 = [\underline{q}_1, \cdots, \underline{q}_{m_u}]$ form an orthonormal basis for the space spanned by $\bar{F}_w$. Note that $g_i = (\underline{q}_i^T \underline{f}_{*w})$ is the length of the projection of $\underline{f}_{*w}$ on $\underline{q}_i$. Thus, the magnitude of g_i is an indication of the importance of the ith actuator to the least squares approximation. The actuator elimination procedure is as follows:

1) rank actuators by g_i values
2) eliminate actuator with lowest g_i value
3) calculate the least squares residual vector, $\underline{r}_w$, for the remaining set

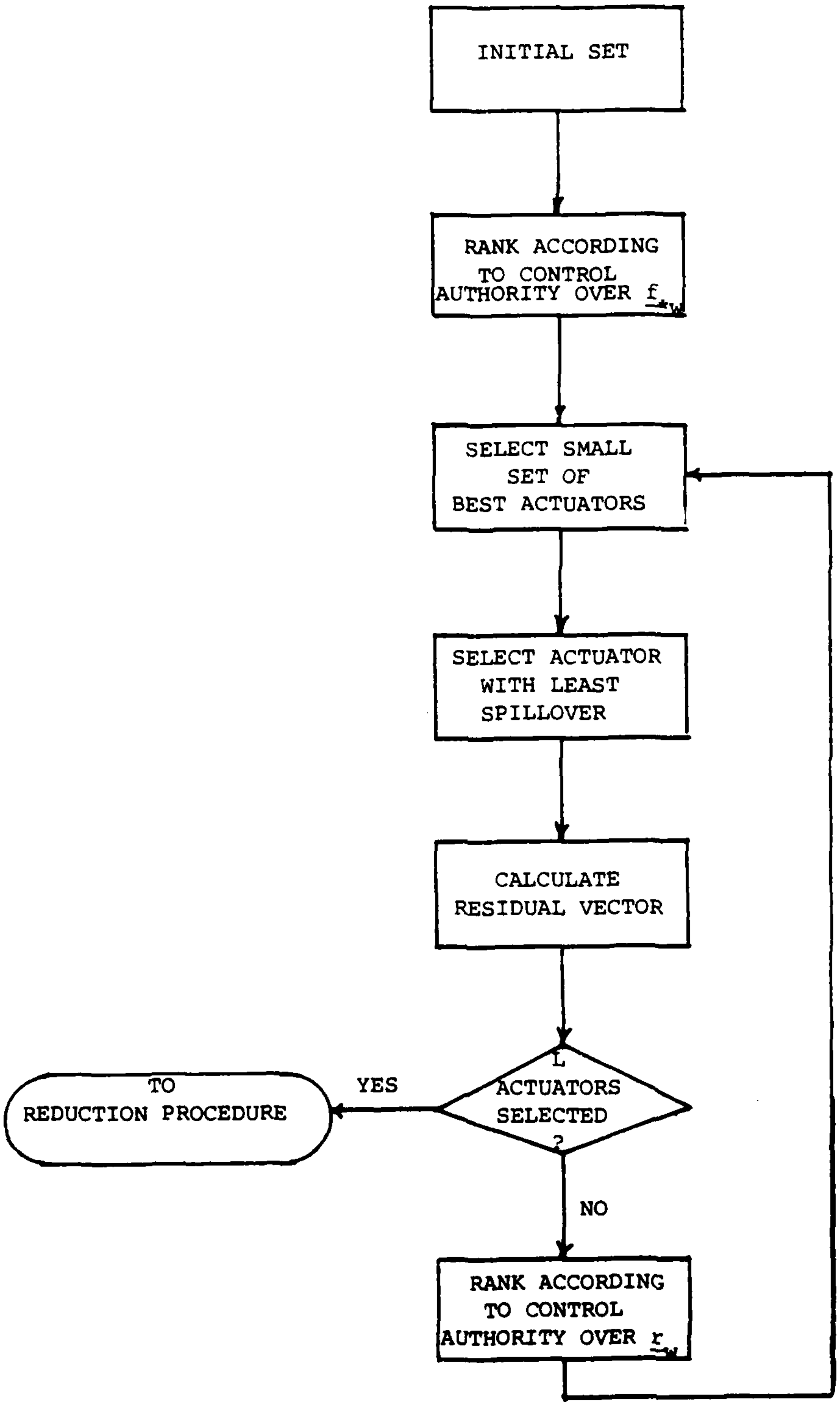

Figure 5-4 Residual Matching Procedure With Spillover Incorporated

4) if $|r_w|$ is less than some ε then eliminate another actuator

5) if $|r_w|$ is greater than some ε then add last actuator eliminated back to set and stop.

ε is the criteria for $|\underline{r}_w| \approx 0$. In this study ε is chosen as 1.0×10^{-6}, this being the approximate accuracy of single precision computations.

5.5 Augmenting the Initial Set

In the actuator reduction procedure above, it is possible to identify modes which are poorly controlled. Inspection of the terms in the residual vector, $\underline{r}_w$, will indicate poorly controlled modes. If some of the terms in $\underline{r}_w$ are greater than ε, then no reduction of the set will be possible. Thus, it is desirable to find actuator locations that will provide adequate control of these modes. These locations are added to the initial set and the selection procedure reaccomplished.

The selection of the locations for such actuators can be aided by a visual inspection of the vibrating structure simulation (if one is available) and/or the analysis of the mode shape(s). For example, locatins at the peak of a mode shape should provide good control authority over that mode.

5.6 Multiple Performance Criteria

In many cases two or more linear performance criteria must be simultaneously met. For example, in an optical structure, the performance specification may be to minimize line of sight (LOS) error in two directions, say x and y. This situation necessitates some minor modifications to the previous development.

First, the primary modes must be defined in terms of all the performance criteria. This leads to a reevaluation of the weighting matrix $\bar{D}$. Recall that the elements of the diagonal $\bar{D}$ matrix were the approximate contribution of each mode to the overall performance. Thus,

an overall performance criteria must be defined. In the LOS error example above, overall LOS error can be written

$$\mathrm{LOS} = \sqrt{(\mathrm{LOS}_x)^2 + (\mathrm{LOS}_y)^2}$$

If the intra-mode interaction is small, it is reasonable to approximate the contribution of the ith mode to the mean square performance, l_i as

$$l_i = (\underline{f}_{*x})_i^2 \, (\underline{\eta}_{ms})_i + (\underline{f}_{*z})_i^2 \, (\underline{\eta}_{ms})_i$$

where $\underline{f}_{*x}$ and $\underline{f}_{*y}$ are the performance (LOS) node shapes for the x and y directions and $\underline{\eta}_{ms}$ is a vector of mean square modal amplitudes for the uncontrolled system. Thus the elements of the $\bar{D}$ matrix, d_{ii}, are given by

$$d_{ii} = l_i w_i$$

where w_i=1 for primary modes and 0 for residual modes.

No modifications are required to use the maximum norm selection procedure. However, several modifications are required to use the residual matching procedure. The residual matching procedure is designed to select L actuator node shapes to match each performance node shape. Thus, as many as 2L actuators could be selected. Some duplication in the actuators selected to match each performance measure is expected and in some cases the selections would be identical. In those cases where more than L actuators are selected, dependent actuators must be eliminated from the set. The suggested procedure is to reduce this set via the maximum norm technique.

The final modification is in the actuator set reduction technique. Here, the elements of g must be evaluated for each performance criteria before an actuator can be chosen for elimination.

CHAPTER 6

100 METER SCE BEAM EXAMPLE

6.1 Physical Description

The first actuator placement study is devoted to a 100 meter space construction experiment (SCE) beam[19] shown in Figure 6-1. The SCE beam is designed to be deployed from the space shuttle cargo bay and will be a test bed for various LSS experiments. The SCE beam is of diamond truss construction, is rigidly attached to the space shuttle, and has a 250 kg tip mass. Additional properties are given in Appendix A.

6.2 Finite Element Analysis

The beam is modeled as having 61 elements connected at 54 node points. Node locations and element connections data are tabulated in Appendix A. The finite element model is based on 10 vibrational modes and 6 rigid body modes. Open loop vibration frequencies are listed in Table 6-1 and plots of the mode shapes are contained in Appendix A.

6.3 Disturbance Description

For the purposes of this study, two white noise disturbances are applied to node 39, one is oriented in the x direction and the other in the y direction. Each disturbance is zero mean and has a variance of 800 nt^2.

6.4 Control Objective

The control system (i.e. actuator placement and controller design) objective is to minimize tip (node 7) movement in both the

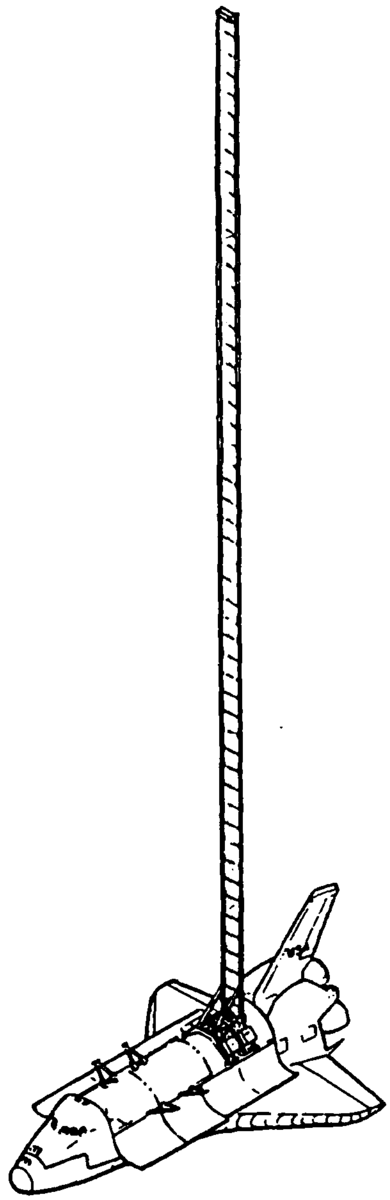

Figure 6-1 Space Construction Experiment Beam

x and y directions. In this case the performance node shapes are identical to the node shapes for displacement in the x and y direction at node 7. The objective is to control the tip movement to the following mean square steady state bounds:

$$x_{ms} \leq 7 \times 10^{-5} m^2$$

$$y_{ms} \leq 9 \times 10^{-5} m^2$$

6.5 Open Loop Characteristics

The beam is modeled as having a damping ratio of .001 for each mode. The open loop characteristics of the beam when subjected to the disturbances are listed in Tables 6-1 and 6-2. The mean square tip movement in the x direction is 0.15 m^2 and 0.048 m^2 in the y direction.

6.6 Controller Design

Actuator placement strategies are evaluated via the performance of a designed controller. The approach taken here is to design a constant gain state feedback regulator and a constant gain Kalman filter using the LQG control philosophy. The controller is based on the primary modes only. The primary mode state equations are

$$\dot{\underline{x}}_p = \bar{A}_p + \bar{B}_p\underline{u} + \bar{\Gamma}_p\underline{d}$$

$$\underline{y} = \bar{C}_p\underline{x}_p$$

where all terms are as defined in Chapter 3. In addition, tip movement can be written

Table 6-1 Open Loop Poles and Vibration Frequencies

REAL	IMAG	DAMPING	FREQUENCY
-5.410687330E-04	5.410684625E-01	1.000000000E-03	5.410687330E-01
-7.150722150E-04	7.150718575E-01	1.000000000E-03	7.150722150E-01
-5.874783520E-03	5.874780583E+00	1.000000000E-03	5.874783520E+00
-7.403243060E-03	7.403239358E+00	1.000000000E-03	7.403243060E+00
-1.818135070E-02	1.818134161E+01	1.000000000E-03	1.818135070E+01
-2.007872010E-02	2.007871006E+01	1.000000000E-03	2.007872010E+01
-2.334321590E-02	2.334320423E+01	1.000000000E-03	2.334321590E+01
-2.572767640E-02	2.572766354E+01	1.000000000E-03	2.572767640E+01
-3.616505430E-02	3.616503622E+01	1.000000000E-03	3.616505430E+01
-4.659422300E-02	4.659419970E+01	1.000000000E-03	4.659422300E+01

Table 6-2 Open Loop Modal Amplitudes

MODE	Mean Square Amplitude
7	55.
8	44.
9	15.0
10	7.6
11	0.59
12	6.0×10^{-5}
13	0.33
14	0.016
15	4.9×10^{-3}
16	5.0×10^{-4}

$$\begin{bmatrix} x_{TIP} \\ y_{TIP} \end{bmatrix} = \bar{C}_L \underline{x}_p$$

where $\bar{C}_L$ is a matrix containing the performance node shapes. It is assumed that position sensors are collocated with the actuators.

The regulator gains are selected to minimize the cost J

$$J = \int_0^{\infty} [\underline{x}_p^T \bar{C}_L^T \bar{Q}_W \bar{C}_L \underline{x}_p + \rho \underline{u}^T \bar{R}_W \underline{u}] dt$$

where

$\bar{Q}_W$ is the output weighting matrix penalizing tip movement in the x and y direction

$\bar{R}_W$ is the input weighting matrix

ρ is a scalar multiplier

The optimal regulator gain matrix, $\bar{K}$, is given by

$$\bar{K} = \rho (\bar{R}_w)^{-1} \bar{B}_p \bar{S}$$

where $\bar{S}$ is the solution to the algebraic matrix Riccati equation

$$0 = -\bar{S}\bar{A}_p - \bar{A}_p^T \bar{S} + \rho \bar{S}\bar{B}_p (\bar{R}_w)^{-1} \bar{B}_p^T \bar{S} - \bar{C}_L^T \bar{Q}_w \bar{C}_L$$

Note that each actuator set will have a different $\bar{B}_p$ matrix which requires calculation of optimal regulator gains for each set to be evaluated.

A constant gain Kalman filter is implemented as the estimator. The constant Kalman gain matrix, $\bar{G}$, is given by

$$\bar{G} = \bar{P}\bar{C}_p^T(\bar{R}_n)^{-1}$$

where $\bar{P}$ is the solution of

$$\bar{A}_p\bar{P} + \bar{P}\bar{A}_p^T + \bar{\Gamma}\bar{Q}_n\bar{\Gamma}^T - \bar{P}\bar{C}_p^T(\bar{R}_n)^{-1}\bar{C}_p\bar{P} = 0$$

and

$\bar{Q}_n$ is the plant noise variance matrix

$\bar{R}_n$ is the sensor noise variance matrix

Note that sensor noise is not included in the problem formulation. The sensor noise variance matrix, $\bar{R}_n$, is used as a design parameter in this problem.

The controller designed for the SCE beam is based on the following values for the weighting matrices and noise covariances.

$$\bar{Q}_w = \begin{bmatrix} 100 & 0 \\ 0 & 200 \end{bmatrix} \qquad \bar{Q}_n = \begin{bmatrix} 800 & 0 \\ 0 & 800 \end{bmatrix}$$

$$\bar{R}_w = \begin{bmatrix} 1 & 0 \\ 0 & 1 \end{bmatrix} \qquad \bar{R}_n = \begin{bmatrix} 1\times10^{-4} & 0 \\ 0 & 1\times10^{-4} \end{bmatrix}$$

ρ is a design variable that is selected for each actuator set such that the controller meets design specifications.

6.7 Control System Evaluation

The steady state performance of a system must be obtained to evaluate the control system design. Consider a system with the state equation

$$\dot{\underline{x}}_a = \bar{A}_a \underline{x}_a + \bar{\Gamma}_a \underline{w}$$

where

$\bar{A}_a$ can represent open or closed loop dynamics

$\underline{x}_a$ is the appropriate state vector

$\underline{w}$ is a vector of white noise inputs

$\bar{\Gamma}_a$ is the appropriate noise influence matrix

The steady state covariance matrix, $\bar{X}$, is obtained by solving the Liapunov equation in the form[20]

$$\bar{A}_a \bar{X} + \bar{X} \bar{A}_a^T + \bar{\Gamma}_a \bar{Q}_n \Gamma_a^T = 0$$

where $\bar{Q}_n$ is the white noise variance matrix. The system performance is defined as the mean square value of the output, y, given by

$$\underline{y} = \bar{C}_L \underline{x}_a$$

Thus, the mean square performance, $\bar{Y}$, can be expressed as

$$\bar{Y} = \bar{C}_L \bar{X} \bar{C}_L^T$$

The control inputs are defined as

$$\underline{u} = \bar{K}\hat{\underline{x}}$$

where $\hat{\underline{x}}$ is a vector of primary mode states for a full state feedback system. For a system with an estimator, $\hat{\underline{X}}$ is the estimate of the primary mode states. Thus, the mean square control inputs, $\bar{U}$, can be expressed as

$$\bar{U} = \bar{K}\hat{\bar{X}}\bar{K}^T$$

where $\hat{X}$ is the appropriate state covariance matrix.

Given the above formulation, the control system is evaluated as follows:

(1) Select a ρ value such that the primary mode full state feedback system (i.e. regulator but no observer) meets specifications for $\bar{Y}$.

(2) Calculate $\bar{U}$

The above characteristics can be compared for control systems based on different actuator set selections.

6.8 Actuator Placement

With the above preliminaries completed, the actuator selection procedures developed in Chapters 4 and 5 can be applied.

6.8.1 Choosing Initial Set

In an effort to make this a non-trivial problem, actuators are not allowed to be placed on the beam section from node 51 to beam tip, a range of approximately 14 meters. Since the beam has the convenient property that the mode shapes are oriented predominantly in either the x or y direction, placing actuators in off axis directions can be ruled out. The actuators considered are of the point force type. The initial set consists of x and y direction actuators located at nodes 26 through 51. This gives a total of 52 possible actuator locations. Actuator numbers, location, and directions of influence are tabulated in Appendix A.

6.8.2 Primary Mode Selection

The first stop n the reduced order controller design is to select the primary modes. For this system, the modes with the most contribution to tip movement will be selected. The overall tip deflection, m, is given by

$$m = \sqrt{x_{TIP}^2 + y_{TIP}^2}$$

The approximate contribution of each mode to the tip deflection can be calculated. These values are listed in Table 6-3 for the uncontrolled, disturbed beam. Based on these values, modes 7, 8, 9, and 10 are selected as primary modes.

Table 6-3. Mean Square Contributions To Tip Deflection

Mode	$x_{ms}(m^2)$	$y_{ms}(m^2)$	$m_{ms}(m^2)$
7	0.150	1.1×10^{-17}	0.150
8	8.0×10^{-17}	0.0459	0.0459
9	2.2×10^{-14}	2.23×10^{-3}	2.23×10^{-3}
10	1.13×10^{-3}	2.5×10^{-14}	1.13×10^{-3}
11	1.1×10^{-13}	2.8×10^{-5}	2.8×10^{-5}
12	3.2×10^{-23}	2.9×10^{-13}	2.9×10^{-13}
13	1.5×10^{-5}	1.1×10^{-12}	1.6×10^{-5}
14	1.1×10^{-12}	3.5×10^{-8}	3.5×10^{-8}
15	3.2×10^{-15}	9.0×10^{-8}	9.0×10^{-8}
16	9.6×10^{-9}	1.8×10^{-16}	9.6×10^{-9}

As noted in Chapter 4, the selection of the elements in the least squares weighting matrix, $\bar{D}$, is based on the contribution of each primary mode to overall performance. Thus, the elements of the $\bar{D}$ matrix are obtained from Table 6.3. The $\bar{D}$ matrix obtained is

$$\bar{D} = \mathrm{diag}\left(0.150,\ 0.0459,\ 2.23\times10^{-3},\ 1.13\times10^{-3},\ 0,\ 0,\ 0,\ 0,\ 0,\ 0\right)$$

6.8.3 Placement via Maximum Norm

Using the maximum norm selection procedures developed in Chapter 5, the actuator set

51 - 36 - 52 - 33

is obtained. The $\bar{R}$ matrix obtained from the QR factorization procedure is

	51	36	52	33
1)	1.57398E-02	-1.10470E-10	-3.56998E-10	5.83884E-03
2)	0.0	7.43986E-03	2.99312E-03	2.57983E-09
3)	0.0	0.0	4.56074E-03	-1.94172E-09
4)	0.0	0.0	0.0	4.33872E-03

The appropriate $\underline{\alpha}$ vectors for the x and y directions are

$$\underline{\alpha}_x = \begin{bmatrix} -1.18\times10^{-1} \\ 2.13\times10^{-7} \\ 3.06\times10^{-8} \\ 8.61\times10^{-1} \end{bmatrix} \qquad \underline{\alpha}_y = \begin{bmatrix} -2.73\times10^{-7} \\ 9.42\times10^{-1} \\ -3.20\times10^{-1} \\ 8.38\times10^{-7} \end{bmatrix}$$

Actuator locations are plotted on Figure 6-2.

6.8.4 Placement via Residual Matching

In this section the Residual matching procedure with no spillover considerations (i.e. ℓ=1.0) is used to place actuators. The selected set for each direction is

x	y
51	52
39	34
34	51
50	39

This set of 5 actuators (note duplications) is reduced to 4 actuators by the maximum norm procedure. The resulting final set is

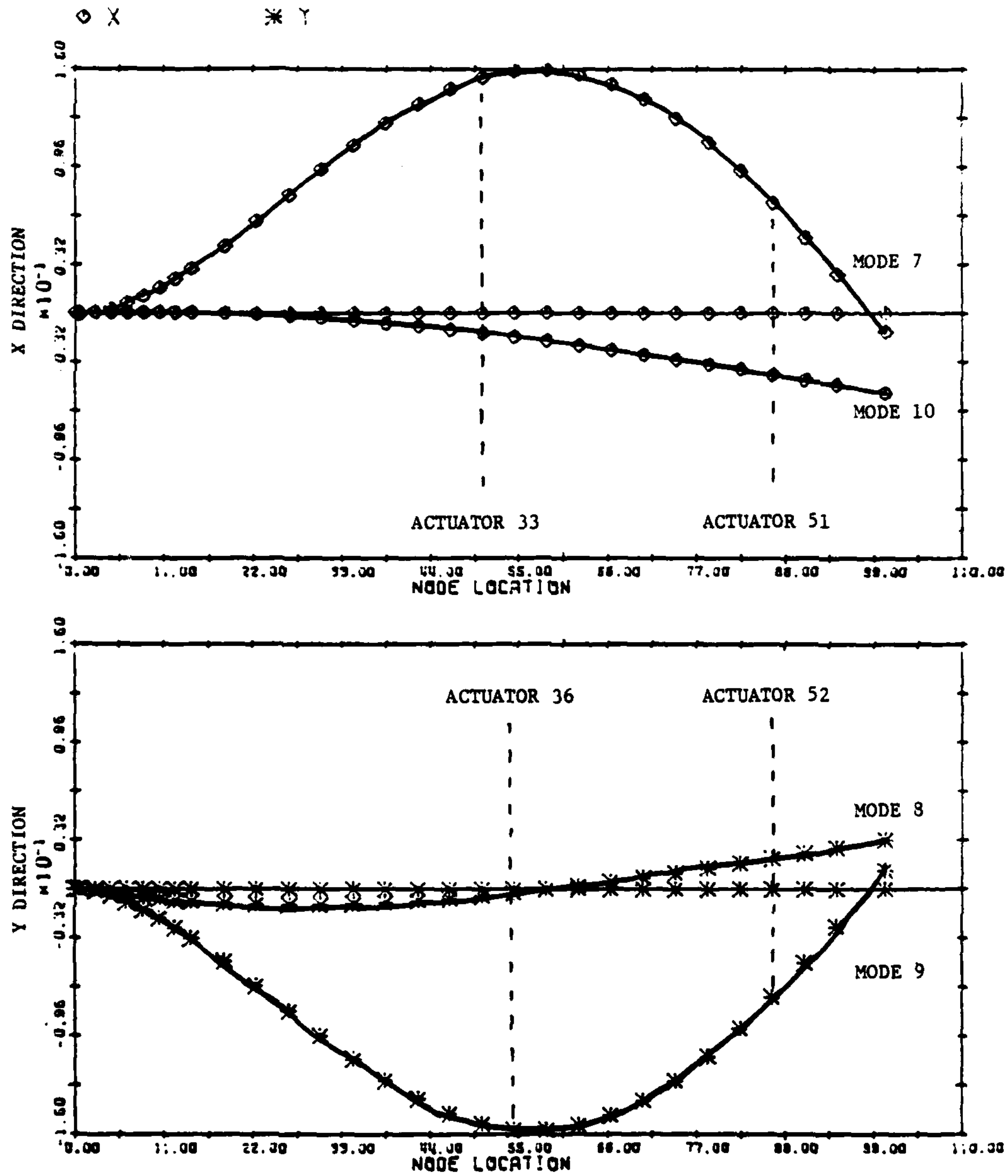

Figure 6-2 Actuator Locations on Primary Mode Shapes
(Selected by Maximum Norm Method)

51 - 34 - 39 - 52

for which the $\bar{R}$ matrix is

	51	34	52	39
1)	1.57398E-02	-1.10470E-10	-3.56998E-10	8.91708E-03
2)	0.0	7.43986E-03	2.99312E-03	1.27244E-09
3)	0.0	0.0	4.56074E-03	-1.84773E-09
4)	0.0	0.0	0.0	3.93113E-03

and the $\underline{\alpha}$ vectors are

$$\underline{\alpha}_x = \begin{bmatrix} -3.37\times10^{-1} \\ 3.42\times10^{-7} \\ 4.91\times10^{-8} \\ 9.51\times10^{-1} \end{bmatrix} \qquad \underline{\alpha}_y = \begin{bmatrix} -4.87\times10^{-7} \\ 9.42\times10^{-1} \\ -3.20\times10^{-1} \\ 9.24\times10^{-7} \end{bmatrix}$$

Actuator locations are plotted on Figure 6-3.

6.8.5 Comparing the Two Methods

The above actuator selections are based on finding the actuator set with the best control authority over the system. Each set matches the intuitive notion that actuators should be placed near peaks in primary mode shapes to give good control authority. A full state feedback controller based on the primary modes is used to compare the two actuator sets.

For the maximum norm set (51-36-52-33), the design parameter ρ is chosen as .0001. this gives a mean square performance of

$$x_{ms} = 6.91 \times 10^{-5}\ m^2$$

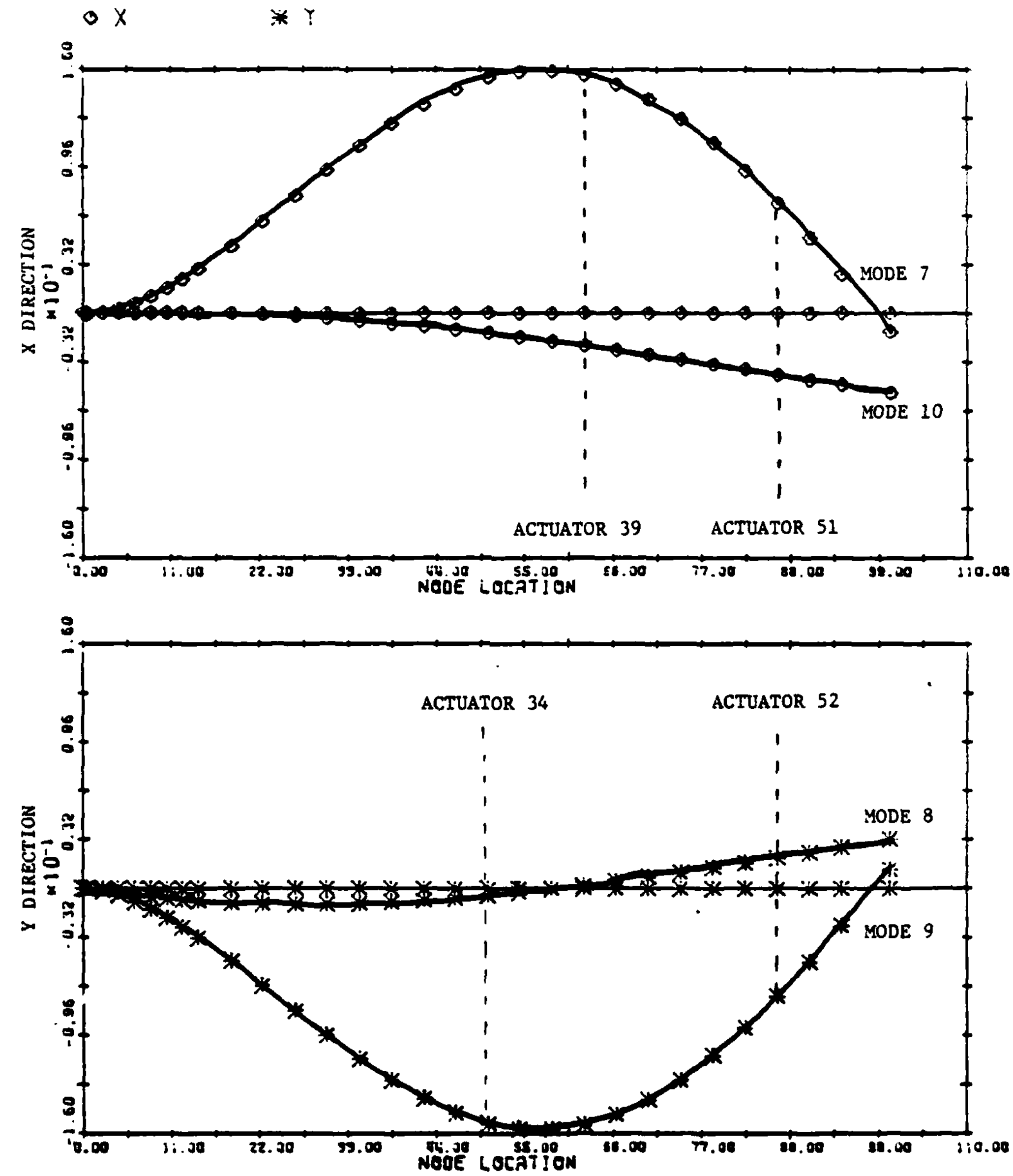

Figure 6-3 Actuator Locations on Primary Mode Shapes
(Selected by Residual Matching Method)

$$y_{ms} = 8.69 \times 10^{-5} \ m^2$$

The control input covariance matrix is

	51	33	52	36
1)	3.520559E+01	2.915335E+01	-1.166614E-05	-1.747576E-06
2)	2.915335E+01	4.683268E+01	-1.122090E-05	2.075952E-05
3)	-1.166614E-05	-1.122090E-05	1.136125E+02	1.848557E+01
4)	-1.747576E-06	2.075952E-05	1.848557E+01	8.968870E+01

A scalar measure of the total force input is the trace of the covariance matrix, $Tr\{\bar{U}\}$. For this set

$$Tr\{\bar{U}\} = 285.33 \ nt^2$$

For the residual matching set (51-34-52-39), the design parameter ρ is again chosen as .0001. This gives a mean square performance of

$$x_{ms} = 6.71 \times 10^{-5} \ m^2$$

$$y_{ms} = 8.64 \times 10^{-5} \ m^2$$

The control input covariance matrix is

	51	39	52	34
1)	2.943699E+01	3.093736E+01	-8.171109E-06	1.007317E-05
2)	3.093736E+01	4.944458E+01	-8.596048E-06	3.242598E-05
3)	-8.171109E-06	-8.596048E-06	1.087050E+02	1.187082E+01
4)	1.007317E-05	3.242598E-05	1.187082E+01	9.478019E+01

For which

$$\mathrm{Tr}\{\bar{U}\} = 282.37 \text{ nt}^2$$

The actuator set selected by intuitive methods (i.e. peaks of mode shapes) is (51-52-37-38). Selecting the design parameter ρ as .0001 gives a mean square performance of

$$x_{ms} = 6.68 \times 10^{-5}$$

$$y_{ms} = 8.82 \times 10^{-5}$$

The control input covariance matrix is

	51	52	37	38
1)	3.102040E+01	-8.179020E-06	2.995857E+01	1.631726E-06
2)	-8.179020E-06	1.171245E+02	-7.931640E-06	2.891552E+01
3)	2.995857E+01	-7.931640E-06	4.816919E+01	1.866040E-05
4)	1.631726E-06	2.891552E+01	1.866040E-05	8.663411E+01

for which

$$\mathrm{Tr}\{\bar{U}\} = 282.65$$

The above results show the residual matching procedure yields a better actuator set than the maximum norm procedure in the sense that slightly better performance was obtained with smaller control force inputs.

6.8.5 Placement via Spillover Considerations

The residual matching procedure was developed with the capability of placing actuators to reduce spillover to selected secondary modes. The selection of secondary modes is not a clear cut procedure. For this study, residual modes that appear most sensitive to spillover effect will be designated as secondary modes.

To determine those modes sensitive to spillover effect, the actuator set 51-39-52-34 is used for a reduced order controller design (regulator and estimator) that is applied to the full 10 mode system. With the design parameter $\rho = .0001$ as utilized above, the system is unstable. Pole locations are listed in Table 6-4. Mode 13 is the unstable mode, and the pole for mode 11 has been shifted very close to the imaginary axis. Designating modes 11 and 13 as secondary modes, an attempt is made to select a set of actuators that will meet system specifications while maintaining a stable system.

Using the residual matching procedure with a limiting factor $\ell=0.9$, the actuator set 51-35-52-36 is obtained. With a design parameter of $\rho=9.0\times10^{-5}$ in the full state feedback system, the mean square performance is

$$x_{ms} = 6.39 \times 10^{-5}$$

$$y_{ms} = 8.19 \times 10^{-5}$$

The control input covariance matrix is

	51	35	52	36
1)	3.432231E+01	3.088186E+01	-9.140142E-06	4.674397E-06
2)	3.088186E+01	5.001754E+01	-7.502096E-06	2.973809E-05
3)	-9.140142E-06	-7.502096E-06	1.188631E+02	1.915437E+01
4)	4.674397E-06	2.973809E-05	1.915437E+01	9.497985E+01

for which $Tr\{\bar{U}\} = 298.18$. This indicates slightly higher force inputs are required to match previous performance levels. However, when this set is used in the design of the reduced order controller, the full order controlled system remains stable. Thus, in this simple example, a reasonable selection of actuator locations has been obtained which achieve the control objectives despite the spillover effect.

CHAPTER 7

SUMMARY AND CONCLUSIONS

7.1 Summary

The purpose of this study was to develop a method of actuator placement to allow vibration control of large spce structures. Previously developed techniques have tended to be computationally intensive and thus are not easily applicable to high order systems. The methods for actuator placement presented in this study are readily extended to high order sysems and showed much promise when applied to a simple large space structure.

With the system equations written in modal coordinates, vectors of displacements associated with both actuator and system performance could be developed. These were termed node shapes. The actuator placement problem was formulated as a least squares problem where a set of actuator node shapes from an initial set of n actuators.

The first technique initially selected the actuator node shape with the maximum norm. Subsequent actuator node shapes were chosen based on the component of the node shape orthogonal to the space spanned by the previously selected set. The orthogonal component of each node shape was calculated and the component with the maximum norm was added to the actuator set. This method was termed the maximum norm technique.

The second technique initially selected the actuator node shape with the largest absolute projection along the performance node shape. The least squares residual vector could then be calculated and subsequent selections were based on the actuator node shapes absolute projection along the residual vector. This method was termed the residual matching technique.

Application of these techniques to a simple beam structure demonstrated that actuator locations chosen were near peaks of primary mode shapes, which is the intuitive concept for actuator location. The maximum norm technique appeared to choose actuator locations that were more orthogonal than those attained by intuitive placement. The residual matching technique appeared to choose actuator locations that were more advantageous to applying control inputs to all the primary modes with a single actuator, rather than an individual mode as in intuitive placement. In other words, the residual matching technique sacrificed some actuator orthogonality in order to attain slightly better control authority over the primary modes. When the control forces required to meet a specific performance objected were examined, the residual matching actuator set gave approximately the same performance as the intuitive actuator set, and both performed better than the maximum norm actuator set.

Position sensors were assumed to be colocated with the actuators and a Kalman filter was added to the control design. The actuator locations used were those selected by the residual matching technique. Analysis of the system poles showed that one of the poles was shifted into the right half s-plane by spillover effect. The residual matching technique was modified to take spillover effect into account in the selection process and actuator locations were reselected. The resulting set required higher control force levels to meet performance specifications in the full state feedback system, but when the system poles were calculated with the Kalman filter in place, all poles remained in the left hand s-plane.

7.2 Conclusions and Recommendations

The above application demonstrates that both selection techniques show promise as actuator placement techniques. In this case the residual matching technique appears to be superior since the actuator set chosen by this technique allows a full state feedback controller to operate with

lower input force levels than the set selected by the maximum norm method. In addition, the residual matching technique has been modified to select actuators so as to limit spillover into selected modes. The application problem demonstrates that proper actuator placement can lead to a stable system that is capable of meeting performance specifications.

The example structure is geometrically simple and is represented by a low order model. Application of the selection techniques to structures with more complex geometry and models of higher order is required to verify the suitability of these placement techniques.

APPENDIX A

SCE BEAM DATA

Table A-1 Truss Characteristics

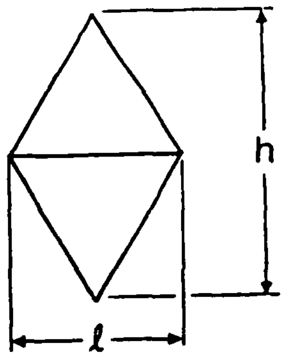

Truss characteristics	
EI pitch	2.0×10^7 N-m^2
EI roll	1.3×10^7 N-m^2
Length	100m
ℓ	2.0m
h	2.83m

Table A-2 Node Locations

NODE	X(m)		Y(m)		Z(m)	
1	0.0		0.0		0.0	
2	0.0		0.0		0.0	
3	0.0		-0.173740005	E+01	0.0	
4	-0.347679996	E+01	-0.110235977	E+01	0.0	
5	0.0		0.173740005	E+C1	0.0	
6	-0.347679996	E+01	0.110235977	E+C1	0.0	
7	0.0		0.0		0.100457199	E+03
8	0.0		-0.110235977	E+01	0.0	
9	0.0		-0.110235977	E+01	0.457199991	E+00
10	0.0		-0.110235977	E+01	0.245718956	E+01
11	0.0		-0.110235977	E+01	0.348488045	E+01
12	0.0		-0.110235977	E+01	0.445718956	E+01
13	0.0		-0.110235977	E+01	0.579119968	E+01
14	0.0		-0.110235977	E+01	0.645718956	E+01
15	0.0		-0.110235977	E+01	0.845718002	E+01
16	0.0		-0.110235977	E+01	0.929487038	E+01
17	0.0		0.110235977	E+01	0.0	
18	0.0		0.110235977	E+01	0.457199991	E+00
19	0.0		0.110235977	E+01	0.245718956	E+01
20	0.0		0.110235977	E+01	0.348488045	E+01
21	0.0		0.110235977	E+01	0.445718956	E+01
22	0.0		0.110235977	E+01	0.579119968	E+01
23	0.0		0.110235977	E+01	0.645718956	E+01
24	0.0		0.110235977	E+01	0.845718002	E+01
25	0.0		0.110235977	E+01	0.929487038	E+01
26	0.0		0.0		0.457199991	E+00
27	0.0		0.0		0.245720005	E+01
28	0.0		0.0		0.445720005	E+01
29	0.0		0.0		0.645720005	E+01
30	0.0		0.0		0.845720005	E+01
31	0.0		0.0		0.104572001	E+02
32	0.0		0.0		0.124572001	E+02
33	0.0		0.0		0.144572001	E+02
34	0.0		0.0		0.184571991	E+02
35	0.0		0.0		0.224571991	E+02
36	0.0		0.0		0.264571991	E+02
37	0.0		0.0		0.304571991	E+02
38	0.0		0.0		0.344571991	E+02
39	0.0		0.0		0.384571991	E+02
40	0.0		0.0		0.424571991	E+02
41	0.0		0.0		0.464571991	E+02
42	0.0		0.0		0.504571991	E+02
43	0.0		0.0		0.544571991	E+02
44	0.0		0.0		0.584571991	E+02
45	0.0		0.0		0.624571991	E+02
46	0.0		0.0		0.664571991	E+02
47	0.0		0.0		0.704571991	E+02
48	0.0		0.0		0.744571991	E+02
49	0.0		0.0		0.784571991	E+02
50	0.0		0.0		0.824571991	E+02
51	0.0		0.0		0.864571991	E+02
52	0.0		0.0		0.904571991	E+02
53	0.0		0.0		0.944571991	E+02
54	0.0		0.0		0.984571991	E+02

Table A-3 Element Connection Data

ELEMENT	NODE1	NODE2
10001	8	9
10002	9	10
10003	10	11
10004	11	12
10005	12	13
10006	13	14
10007	14	15
10008	15	16
20001	17	18
20002	18	19
20003	19	20
20004	20	21
20005	21	22
20006	22	23
20007	23	24
20008	24	25
30001	26	27
30002	27	28
30003	28	29
30004	29	30
30005	30	31
30006	31	32
30007	32	33
30008	33	34
30009	34	35
30010	35	36
30011	36	37
30012	37	38
30013	38	39
30014	39	40
30015	40	41
30016	41	42
30017	42	43
30018	43	44
30019	44	45
30020	45	46
30021	46	47
30022	47	48
30023	48	49
30024	49	50
30025	50	51
30026	51	52
30027	52	53
30028	53	54
30029	54	7
111	3	10
112	3	12
121	4	10
211	5	19
212	5	21
221	6	19
31011	26	9
31012	27	10
31013	28	12
31014	29	14
31015	30	15
31021	26	18
31022	27	19
31023	28	21
31024	29	23
31025	30	24

Table A-4 Actuator Locations

ACTUATOR	DIRECTION	NODE
1)	TX	26
2)	TY	26
3)	TX	27
4)	TY	27
5)	TX	28
6)	TY	28
7)	TX	29
8)	TY	29
9)	TX	30
10)	TY	30
11)	TX	31
12)	TY	31
13)	TX	32
14)	TY	32
15)	TX	33
16)	TY	33
17)	TX	34
18)	TY	34
19)	TX	35
20)	TY	35
21)	TX	36
22)	TY	36
23)	TX	37
24)	TY	37
25)	TX	38
26)	TY	38
27)	TX	39
28)	TY	39
29)	TX	40
30)	TY	40
31)	TX	41
32)	TY	41
33)	TX	42
34)	TY	42
35)	TX	43
36)	TY	43
37)	TX	44
38)	TY	44
39)	TX	45
40)	TY	45
41)	TX	46
42)	TY	46
43)	TX	47
44)	TY	47
45)	TX	48
46)	TY	48
47)	TX	49
48)	TY	49
49)	TX	50
50)	TY	50
51)	TX	51
52)	TY	51
53)	TX	52
54)	TY	52
55)	TX	53
56)	TY	53
57)	TX	54
58)	TY	54

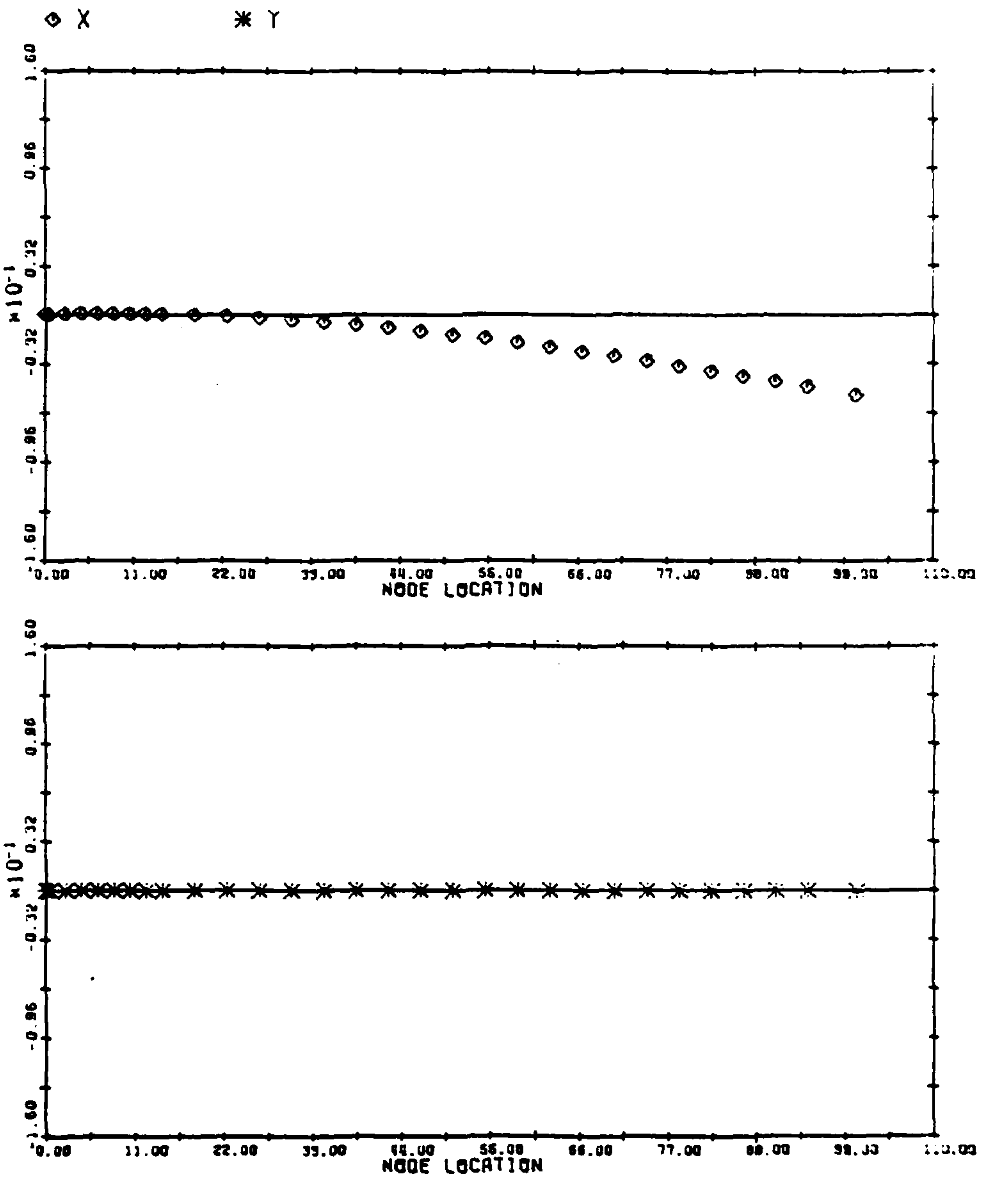

Figure A-1 Mode 7 Mode Shape

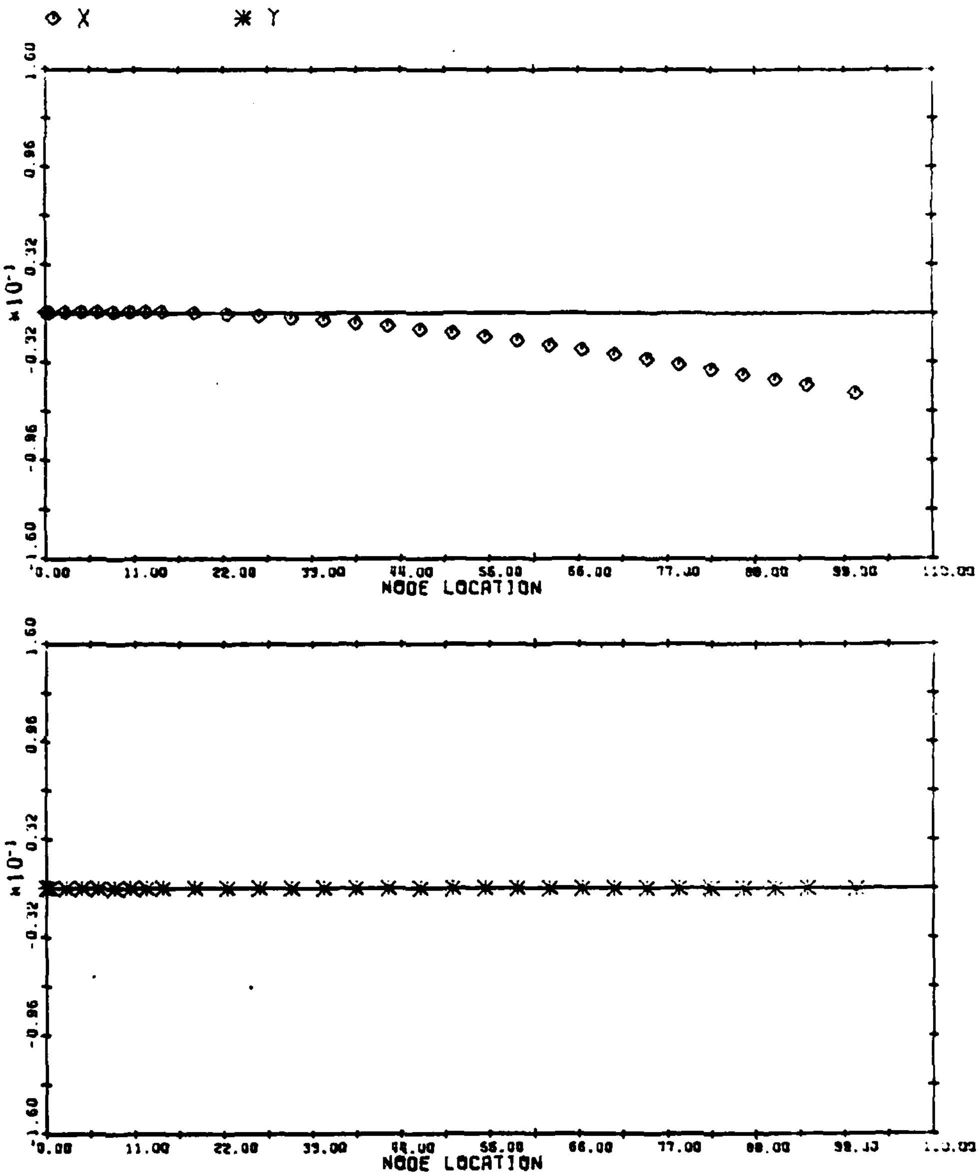

Figure A-1 Mode 7 Mode Shape

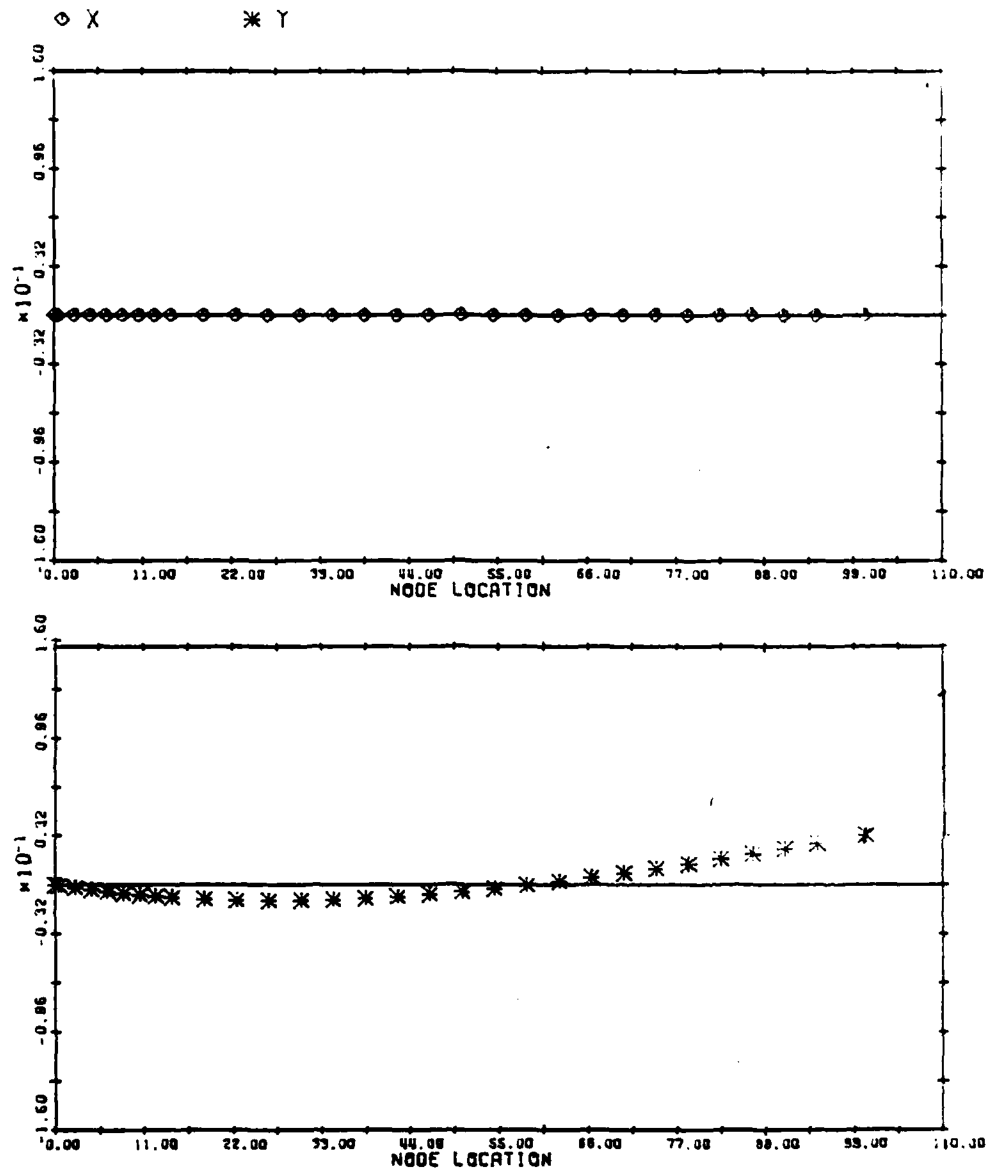

Figure A-2 Mode 8 Mode Shape

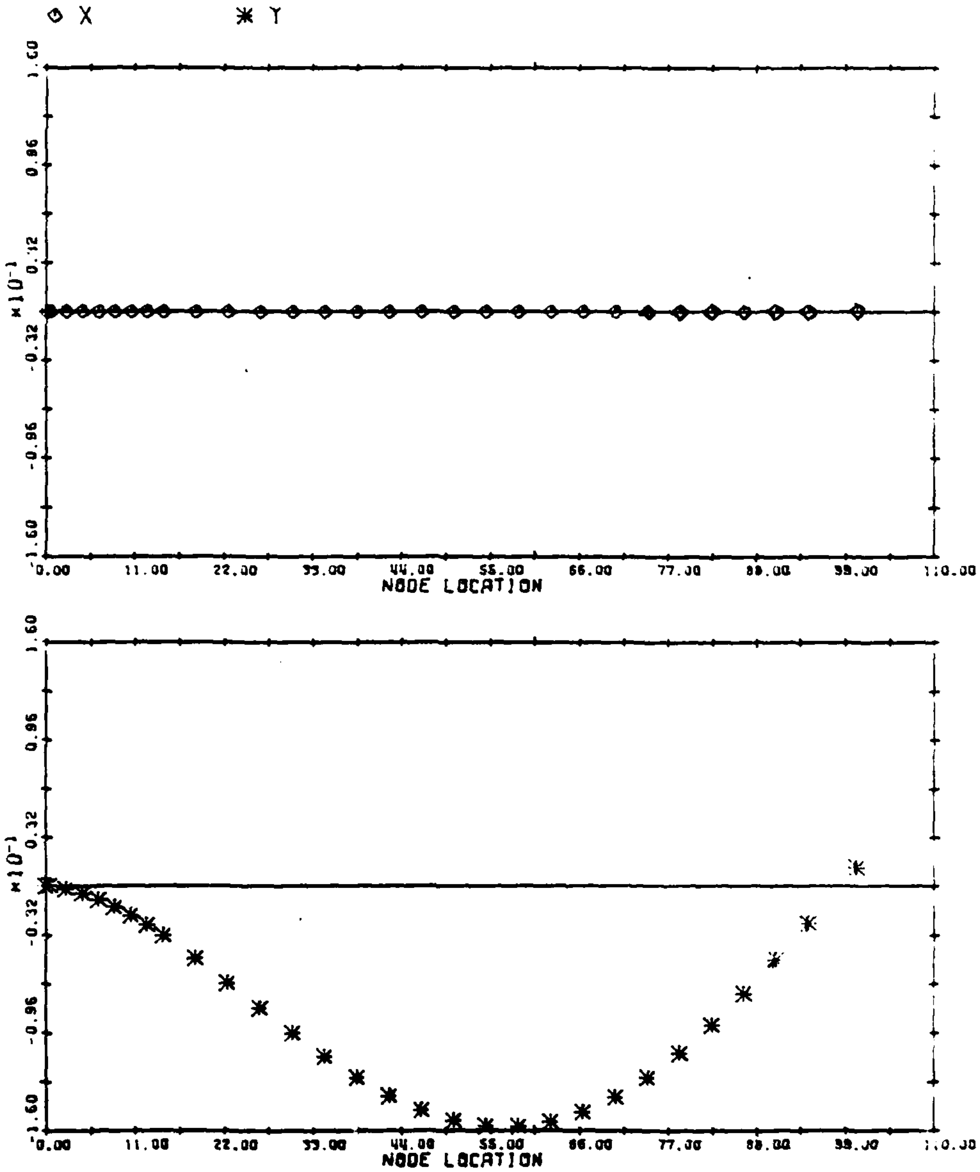

Figure A-3 Mode 9 Mode Shape

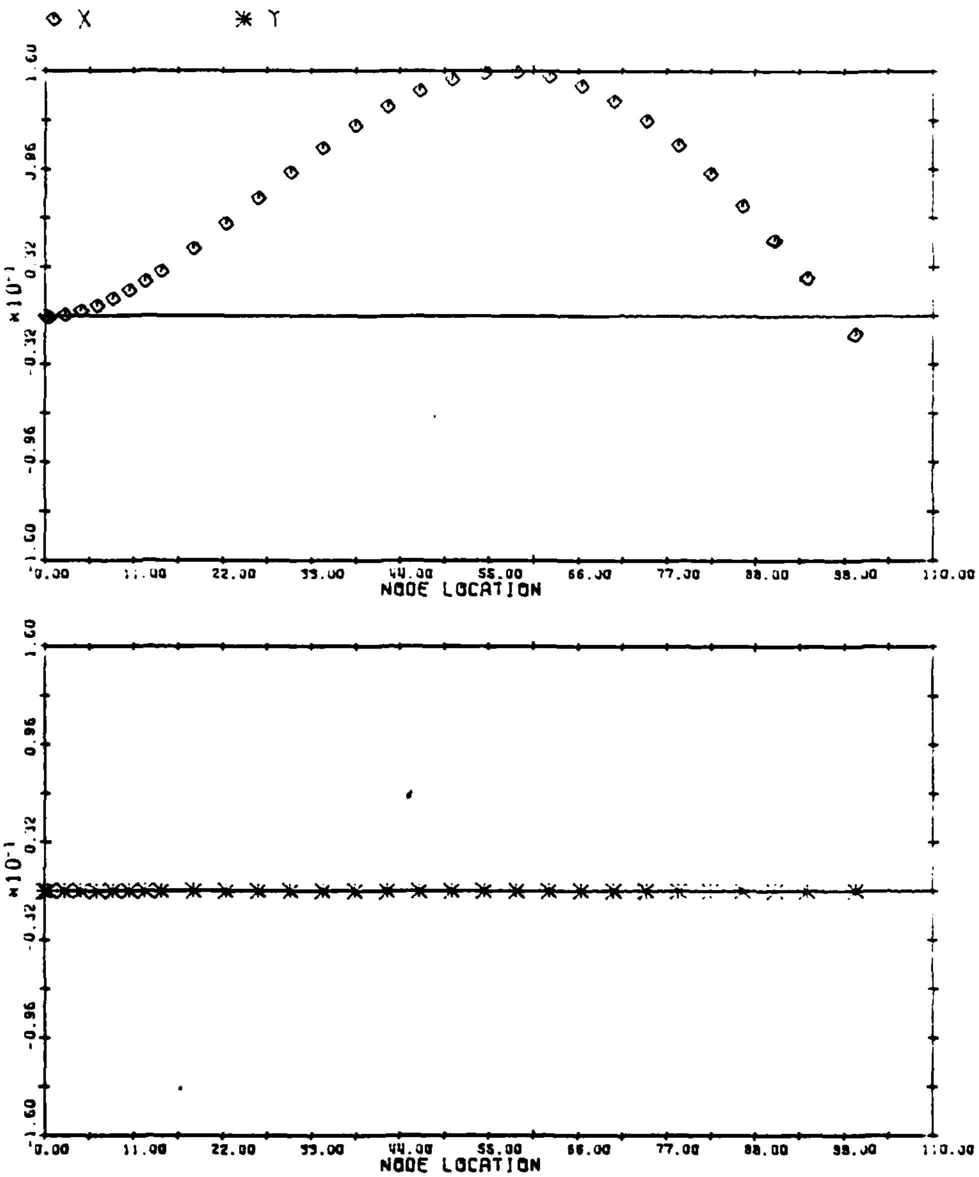

Figure A-4 Mode 10 Mode Shape

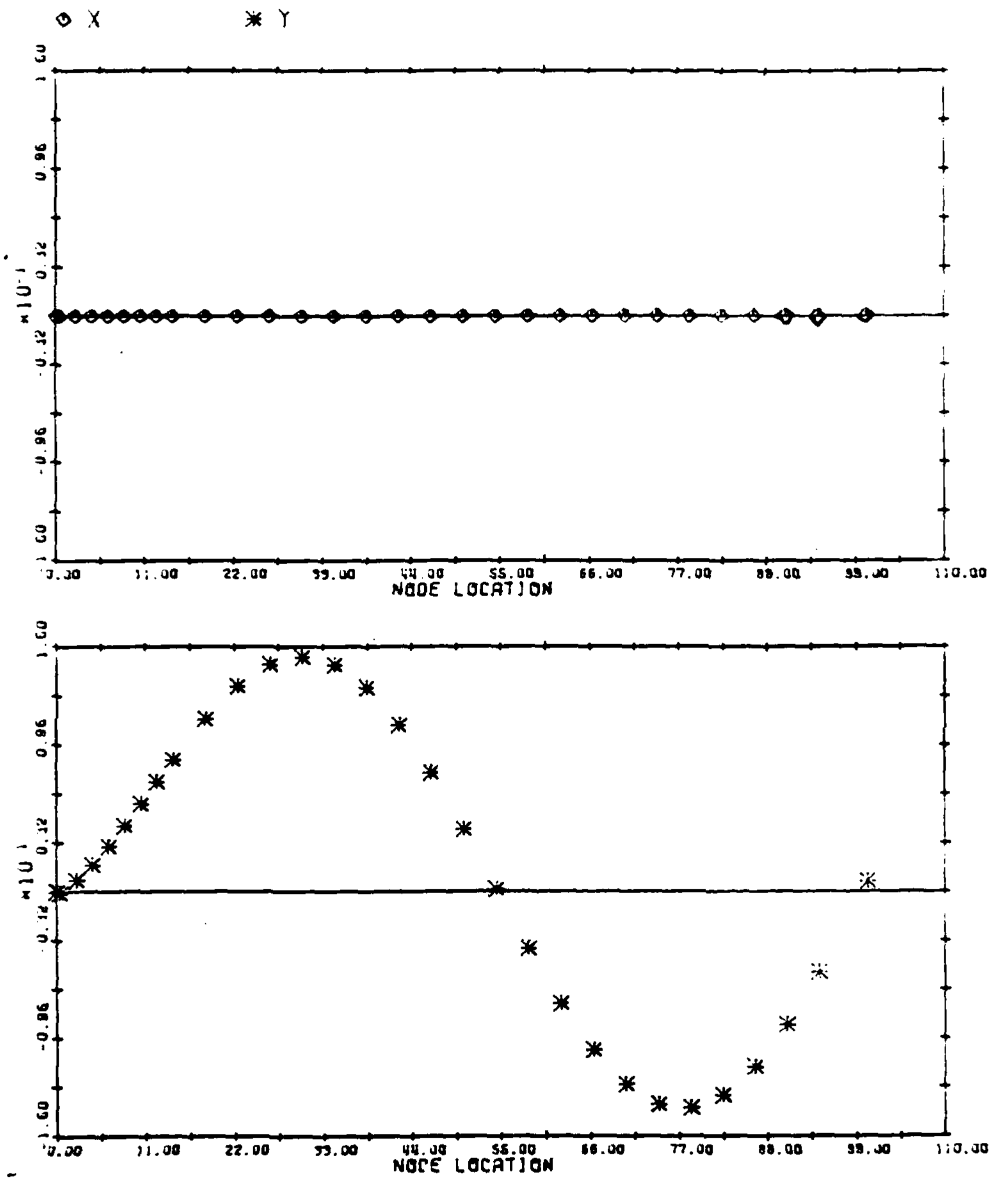

Figure A-5 Mode 11 Mode Shape

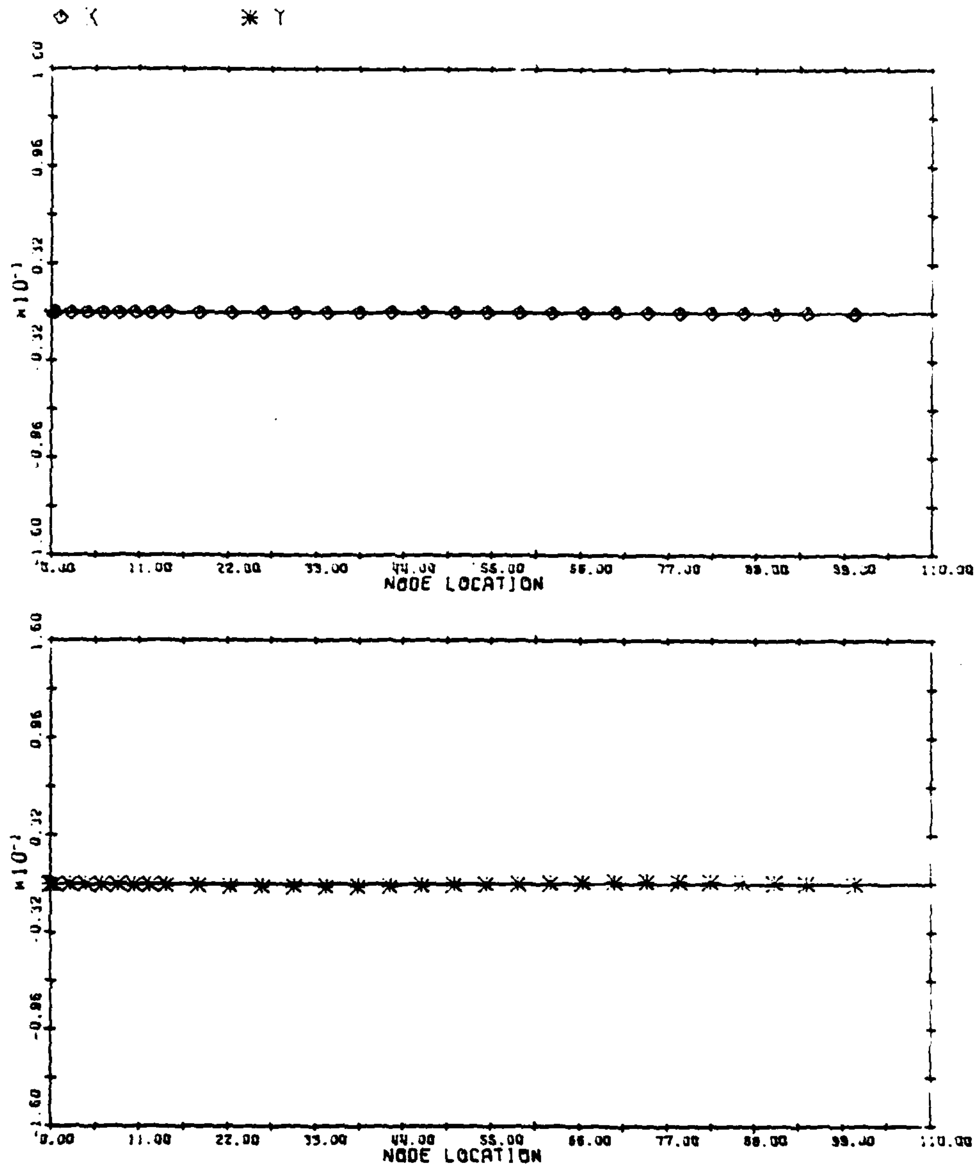

Figure A-6 Mode 12 Mode Shape

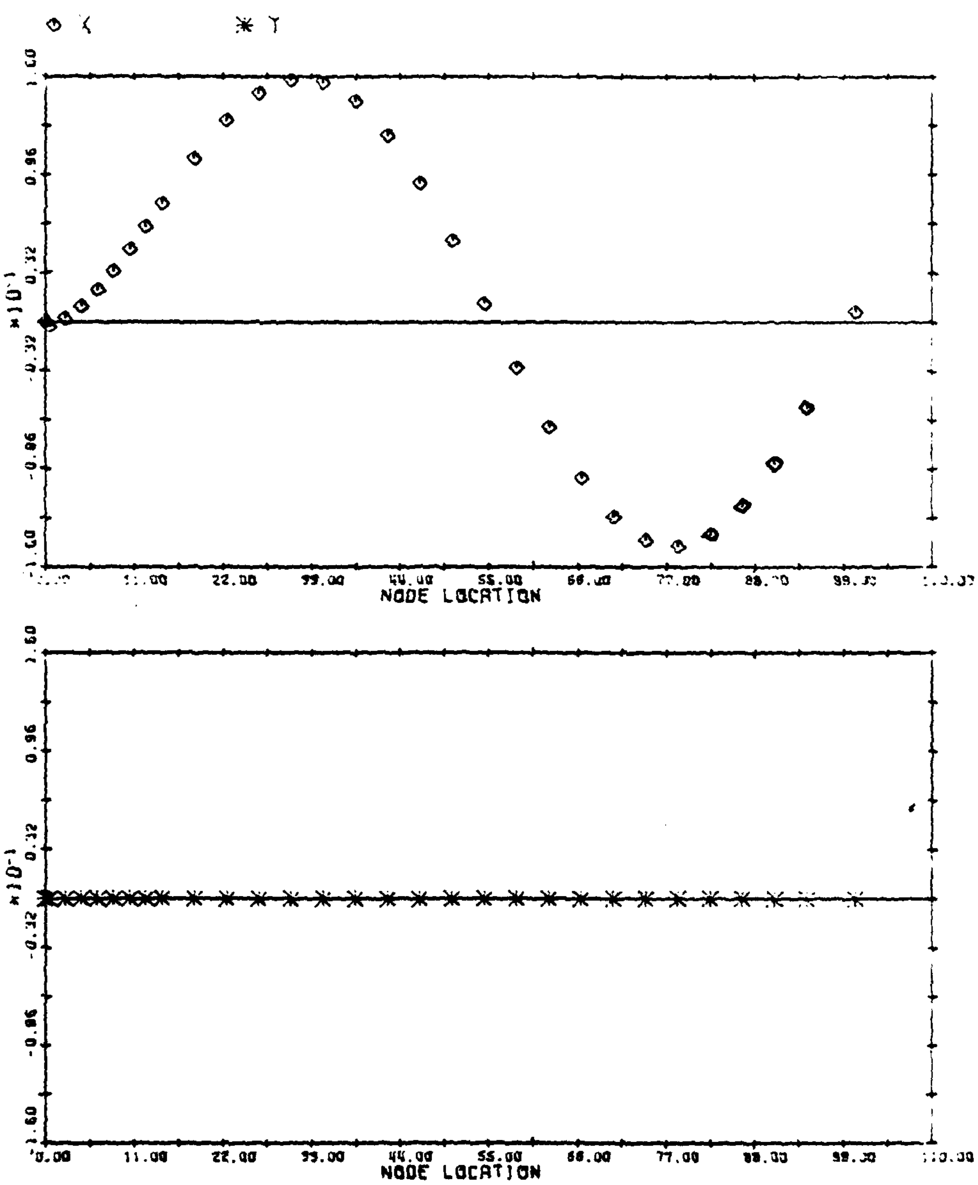

Figure A-7 Mode 13 Mode Shape

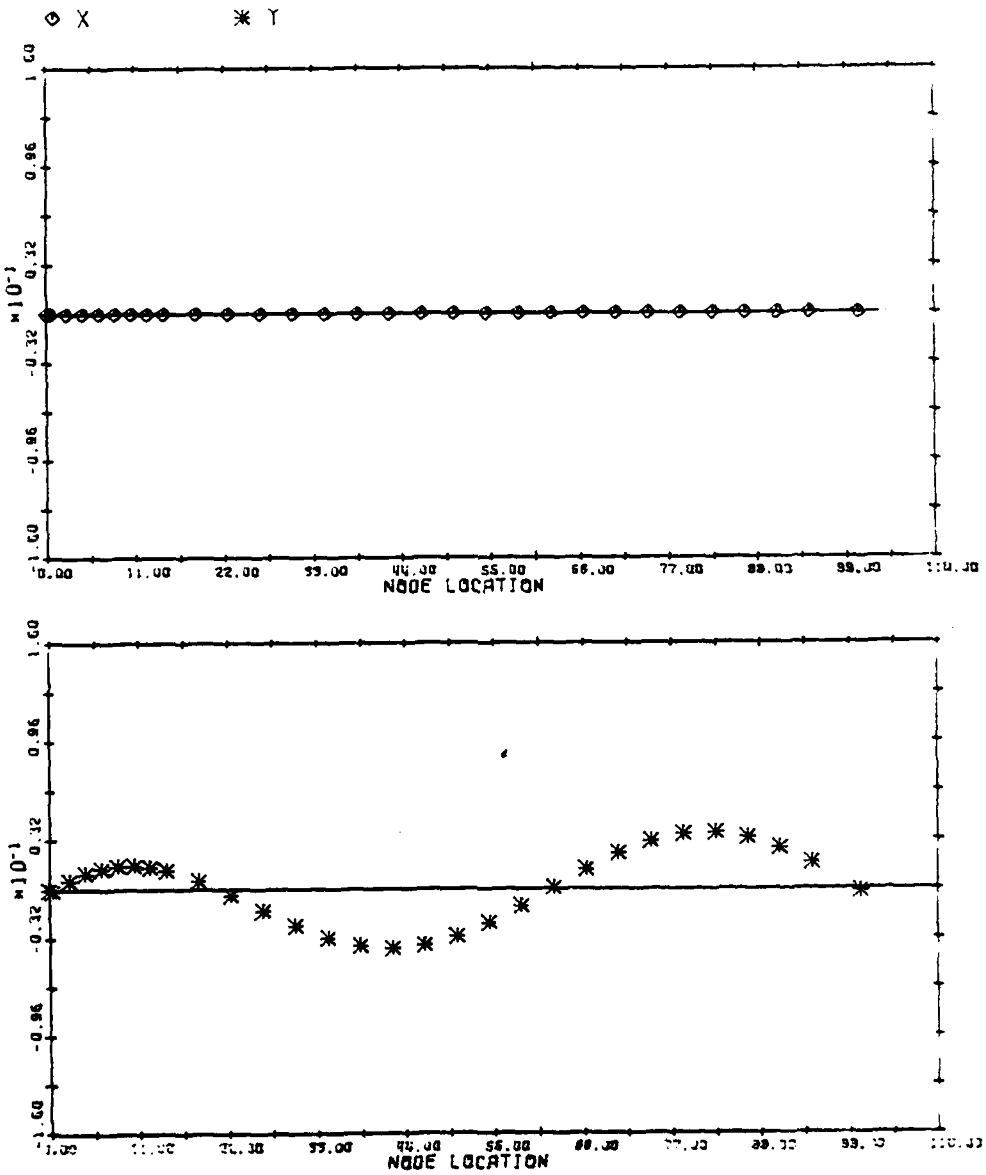

Figure A-8 Mode 14 Mode Shape

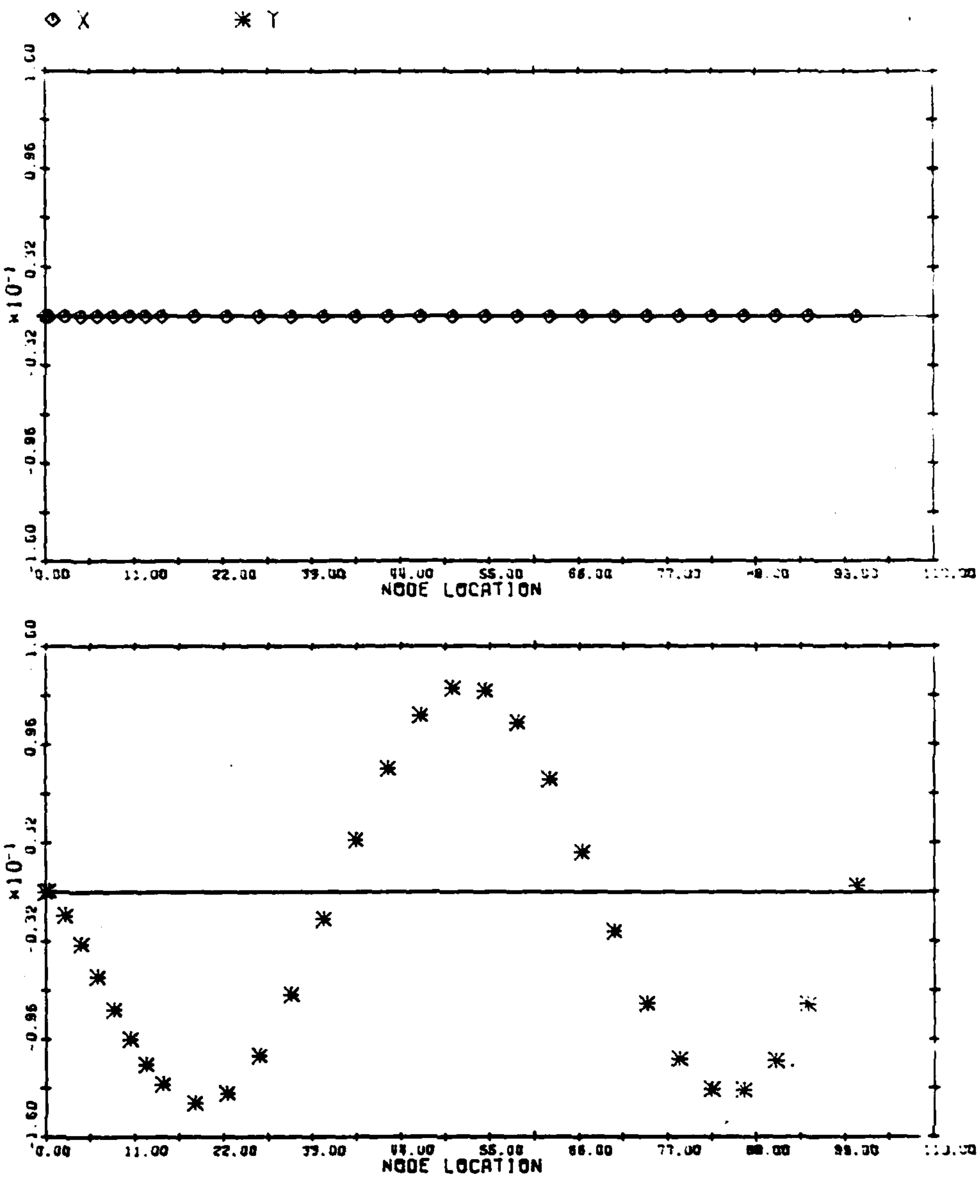

Figure A-9 Mode 15 Mode Shape

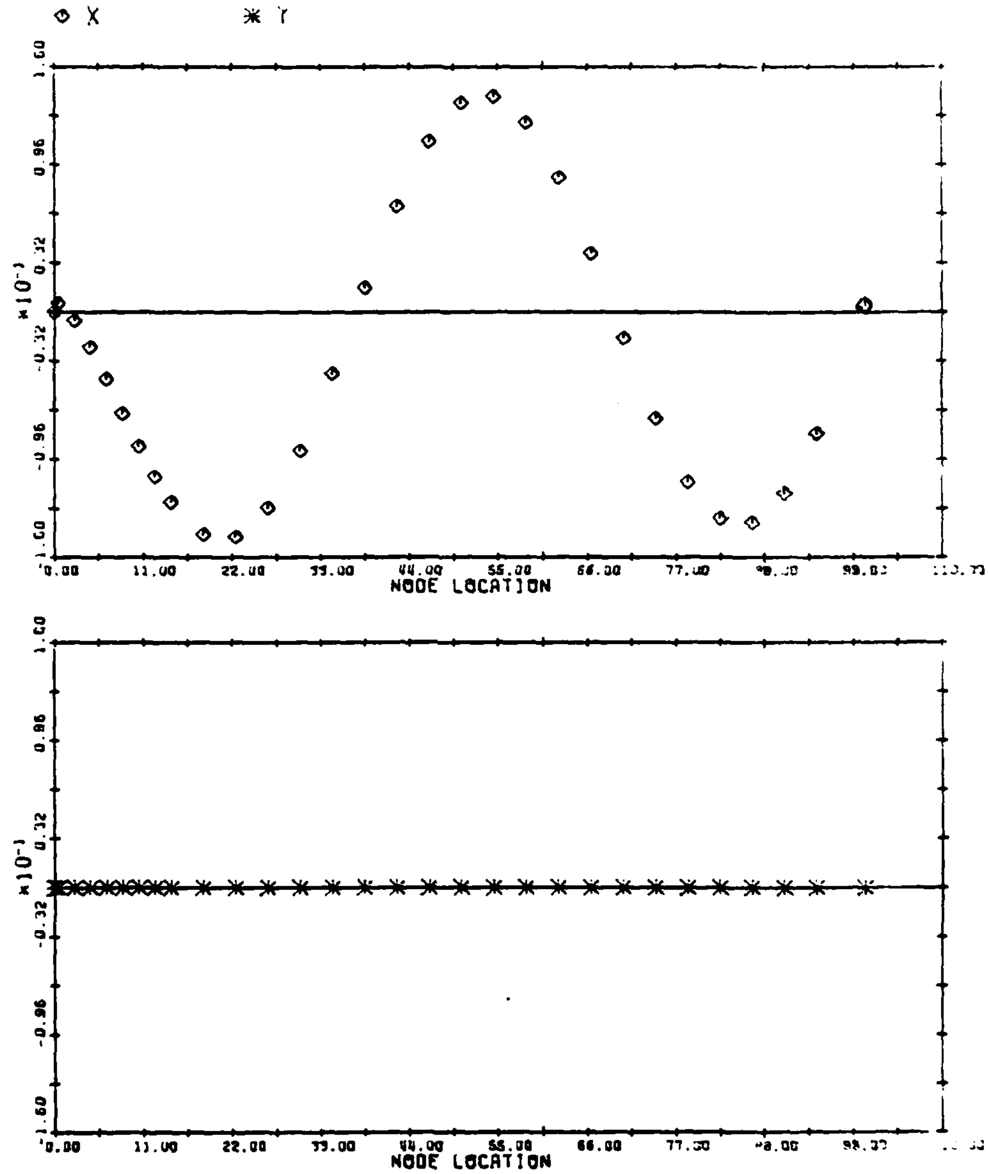

Figure A-10 Mode 16 Mode Shape

LIST OF REFERENCES

1. Henderson, T., "Active Control of Space Structures (ACOSS) Model 2," CSDL Report C-5437, September 1981.
2. Vander Velde, W.E. and C.R. Carignan, "Number of Placement of Control System Components Considering Possible Failures," MIT Space Systems Lab. Report No. 5-82, March 1981.
3. Croopnick, S.R., Y.H. Lin, and R.R. Strunce, "A Survey of Automatic Control Techniques for Large Space Structures," Automatic Control in Space (IFAC), Pergamon Press, New York, 1979, pp. 275-284.
4. Kabamba, P.T., and R.W. Longman, "An Integrated Approach to Optimal Reduced Oder Control Theory," Dynamics and Control of Large Flexible Spacecraft, Proceedings of the Third VPI&SU/AIAA Symposium, 1981 pp. 571-585.
5. Meirovitch, L., H. Baruh, and H. Oz, "A Comparison of Control Techniques for Large Flexible Systems," AAS/AIAA Astrodynamics Specialist Conference, August 1981.
6. Tung, F.C., "Finite Element Models and System Identification of Large Space Structures," Dynamics and Control of Large Flexible Spacecraft, Proceedings of the Third VPI&SU/AIAA Symposium, 1981, pp. 255-267.
7. Balas, M.J., "Active Control of Flexible Systems," Symposium of Dynamics and Control of Large Flexible Spacecraft, Blacksburg, VA, June 1977.
8. Gibson, J.S., "Convergence and Stability in Linear Modal Regulation of Flexible Structures," Dynamimcs and Control of Large Flexible Spacecraft, Proceedings of the Second Symposium (VPI&SU/AIAA), 1979, pp. 51-64.

9. Herther, J.G., Vibration Control of Large Space Structures Using Linear Quadratic Techniques, M.S. Thesis, Draper Report CSDL-T-767, February 1982.

10. Joshi, S.M., and N.J. Groom, "Controller Design Approaches for Large Space Structures Using LQG Control Theory," Dynamics and Control of Large Flexible Spacecraft, Proceedings of the Second Symposium (VPI&SU/AIAA), 1979, pp. 35-50.

11. Arbel, A., "Controllability Measures and Actuator Placement in Oscillatory Systems," International Journal of Control, 1981, Vol. 33, No. 3, 565-574.

12. Muller, P.C., and H.I. Weber, "Analysis and Optimization of Certain Quantities of Controllability and Observability for Linear Dynamical Systems," Automatica, 1972, Vol. 8, pp. 237-246.

13. Juang, J.N., and G. Rodriguez, "Formulations and Applications of Large Space Structure Actuator and Sensor Placements," Dynamics and Control of Large Flexible Spacecraft, Proceedings of the Second Symposium (VPI&SU/AIAA), 1979, pp. 247-262.

14. Viswanathan, C.N., R.W. Longman, and P.W. Likins, "A Definition of the Degree of Controllability - A Criterion for Actuator Placement," Dynamics and Control of Large Flexible Spacecraft, Proceedings of the Second Symposium (VPI&SU/AIAA), 1979, pp. 369-384.

15. Vander Velde, W.E., and C.R. Carignan, "A Dynamic Measure of Controllability and Observability for the Placement of Actuators and Sensors on Large Space Structures," MIT Space Systems Lab. Report No. 2-82, January, 1982.

16. MacNeal, R.H., The NASTRAN Theoretical Manual, The MacNeal-Schwendler Corp. December 1972.

17. Kwakernaak. H., and R. Sivan, Linear Optimal Control Systems, John Wiley and Sons, Inc., New York, 1972.

18. Fogel, E., "Sensor/Actuator Selection, "ACOSS Eleven Second Semi-annual Technical Report, CSDL Report 1583, Volume 2, August 1982.

19. Bryson, A.E. and Hoe, Applied Optimal Control, Blaisdell Publ. Co., Mass., 1975.

20. Dongarra, J.J.,and J.R. Bunch, LINPACK Users Guide, Society for Industrial and Applied Mathematics, 1980.

DAT
FILM